Towards the Implementation of ISFET Sensors for In-Situ and Real-Time Chemical Analyses in Soils: A Practical Review

George Archbold[abc], Carlos Parra[a], Henry Carrillo[d], and Abdul Mouazen[b*]

[a]Department of Electronics, Faculty of Engineering, Pontificia Universidad Javeriana, Bogotá, Colombia

[b]Department of Environment, Faculty of Bioscience Engineering, Ghent University, Coupure Links 653, 9000 Gent, Belgium

[c]Corporación del Laboratorio al Campo, San Andrés Isla, Colombia

[d]Genius Sports, Medellín, Antioquia, Colombia

*E-mail of the corresponding author: Abdul.Mouazen@UGent.be

Abstract

Estimating available nutrients and pH in soils has been considered an essential step to improve soil fertility for better crop growth and yield. Classical or conventional laboratory analyses are time-consuming, expensive and expose chemical agents to the environment, hence, do not fulfil the requirement of high sampling resolution data for Precision Agriculture (PA) applications. Proximal Soil Sensing (PSS) allows generating high-volume data quickly and cost-effectively. A functional technology under PSS is the Ion-Sensitive Field-Effect Transistor (ISFET) sensor, which is based on electrochemical principles and can estimate pH and available nutrients in soils. However, their use in PA is limited, compared to other disciplines, e.g., biomedical sciences. This paper presents a state-of-the-art review of ISFET sensors and their use in soil nutrients and pH analyses, highlighting the technical potential and limitations related to implementation. The review focuses on essential concepts (e.g., basic operation principle, algorithms, sensor representations, behavioral model, and simulation example), performance characteristics (e.g., relevant variables, non-idealities, and electronic instrumentation), application examples in PA, and some perspectives of implementation. The goal is to raise awareness of ISFET sensors in the agriculture community and to offer a starting point to those who plan to adopt ISFET sensors in PA.

Keywords

Precision agriculture, In-situ, “Real-time”, Soil chemical analysis, ISFET Sensor, Electrochemical sensors, readout circuit, Circuit simulation.

1. Introduction

An essential requirement in soil fertility management is the chemical analysis that should provide necessary data for optimal fertilization according to crops’ needs. Key soil fertility attributes needed to establish a correct fertilizer recommendation to improve plant growth are organic carbon, pH, macronutrients, and micronutrients (Lin et al., 2008; Ali et al., 2020). However, the classical laboratory methods of soil analyses of the named soil fertility parameters are time-consuming, expensive, require expert operators, and use chemical agents that are harmful to the environment. This way, only a limited number of soil samples can be analyzed, e.g., one sample per field or one sample per hectare in the best scenario (Guerrero et al., 2021). Therefore, variable rate fertilization (VRF), one of the Precision Agriculture (PA) solutions, based-on the laboratory analyses is of limited benefits as the spatial variability with high resolution is not a viable solution. Therefore, in-situ and “real-time” measurement methods of the named soil fertility parameters that allow for quick analyses and decisions in the field are suitable to implement VRF solutions, aiming at higher crop yield, more efficient use of fertilizers and reduced environmental footprint. Fortunately, this can be achieved by implementing Remote Sensing or Proximal Soil Sensing (PSS) technologies, or the fusion of several technologies. Today measurement platforms that enable on-site and on-the-go measurements by a mobile or non-mobile system are available for research and commercial applications (Kuang et al., 2012). These sensor technologies should, however, be relatively cheap, quick, precise, reliable, and portable, without use of chemical agents.

PSS is defined as the use of field-based sensors to obtain signals from the soil when the sensor detector is in direct contact with or close to (within 2m) the soil (Behera et al., 2022). PSS technologies provide raw data (signals) corresponding to physical measures, which can be related to soil types or soil properties. According to Viscarra Rossel et al. (2011), PSS may be defined by the measurement type (invasive [in-situ or ex-situ] or non-invasive), the energy source (active or passive), operating method (stationary or mobile), and the inference of soil property measurement (direct or indirect). Also, these sensors can be electrochemical, optical, radiometric, mechanical, and pneumatic (Ji et al., 2019). The electrochemical and spectral sensors are favorable options to measure soil nutrients. Particularly, electrochemical sensors enable the detection of ion concentrations in solutions obtained from soil samples. Guerrero et al. (2021) reported that electrochemical sensors are suitable for measuring soil mineral nitrogen. However, the need for sensor cleaning after each measurement and the preparation of soil solution to be measured by the sensor are the main challenges that need to be solved for successful integration of these sensors into on-the-go measurement platforms (also known as on-line platforms). Other challenges, include the lag time the need to remove debris from the soil samples, and the extraction should be filtered before the measurement. Apart from the on-the-go systems, on-site prototypes allow real-time collection of data overtime at selected points in the field (Lehmann and Grisel, 2014). Both systems can make use of Ion-Selective Electrode (ISE) or Ion-Sensitive Field Effect Transistor (ISFET) electrochemical sensors. In this work, the focus is made on the ISFET sensor, which is discussed comparatively with ISE.

ISFET is a versatile small sensor technology with many potential applications in several sectors, including the estimation of soil pH and available nutrients. The first applications of the ISFET sensor were in the context of the neurophysiological measurements in 1972 by Piet Bergveld, who was the creator of these solid-state devices. In his research, Bergvled demonstrated the capability of these sensors for measuring ion activities in biological and electrochemical environments(Bergveld, 1970). Although these sensors have achieved popularity thanks to its use in biomedical applications such as Deoxyribonucleic Acid (DNA) sequencing (Moser et al. 2016), there have been some attempts in the last three decades to exploit its enormous potential in PA. However, more research and exploration of the potential of ISFET for PA applications is required. For example but not limited to, future research needs to explore their potential for integration into mobile platforms, to establish consolidated macronutrient mapping systems in large agricultural lands (Chen and Chan 2008; Sibley et al. 2009). Although this is a simple statement, its realization requires answering several research and technical questions, concerning, robustness, repeatability, durability, and accuracy. Given their portability and adaptability to custom-made electronic systems, the establishment of Internet of Things (IoT) based systems could be highly viable (Archbold et al., 2019). However, it is necessary to establish frameworks that allow ISFET sensors to be fused with other sensors, enable telecommunications, and promote practical applications (Archbold et al., 2020).

Despite the proven potential of ISFET to measure ion concentrations directly in ion solutions, their adoption for soil analyses in PA context is rather limited. Literature shows few review reports about the use of ISFET among other sensor technologies for agricultural and environmental applications (Kashyap and Kumar, 2021; Elli et al., 2022; Nadporozhskaya et al., 2022; Hamimed et al., 2023) including PA (Yin et al., 2021). However, to the best of our knowledge there is no literature study dedicated to ISFET, focusing on understanding the electronic instrumentation and non-idealities and their effect on in situ applications in PA. The aim of this paper is to provide an overview of the ISFET sensors, including the basic principles, modeling and simulation needs, non-ideal effects, and electronic instrumentation requirements. The review also discuss the ISFET sensor's relevance for analyzing soil nutrients and pH, including various Digital Agriculture (DA) application examples reported in the literature.

During analyzing and reviewing the literature, a framework introduced by Templier and Paré (2015) was adopted. The set research objective was to find an evidence of the ISFET sensor use for soil analysis and its main electronic and instrumentation requirement. Then, the following systematic steps were implemented in this work: 1) searching existing literature in ScienceDirect, Web of Science, IEEE Explore, etc., related to ESFET and their use in soil analysis, 2) screening most relevant works for inclusion and further analysis, and 3) assessing the quality of these screened studies, and extracting and analyzing relevant information.

2. Fundamentals of Ion-Sensitive Field-Effect Transistor (ISFET)

2.1. Theory and definition

The basic working principle of electrochemical sensors relays on selectively to a particular ion in aqueous solutions according to a logarithmic relationship between the ionic activity and electric potential. ISFET sensors require recognition elements, i.e., ion-sensitive membranes, integrated with a reference electrode, which enables a chemical response (ion concentration) to be converted into a potential electrical signal (Eggins, 2002). ISFET is an electronic device capable of measuring ions in an electrolyte solution. The device is similar to the Metal-oxide-semiconductor Field-effect transistor (MOSFET), but with some fundamental differences (Figure 1). These differences are: (1) the device in ISFET can modulate the threshold voltage through the oxide/solution interface potential, (2) the device in ISFET has the gate connection separated from the chip and includes a reference electrode (typically Ag/AgCl) inserted in an aqueous solution, which is in contact with the gate membrane.

A standard operation mode for MOSFETs corresponds to the non-saturated region (ohmic or linear region). It represents an analogy to understand the operation of ISFET device, since the saturated region is not relevant for the initial ISFET analysis. The drain current in the non-saturated region (I_d), given by Equation (1), represents the behavior of both devices.

$$I_d = \beta\left[(V_{gs} - V_t)V_{ds} - \frac{1}{2}{V_{ds}}^2\right] \forall\, V_{ds} \leq V_{gs} - V_t \tag{1}$$

Where: V_{gs} is the gate-source voltage, V_{ds} is the drain-source voltage, V_t is the threshold voltage and $\beta = C_{ox}\mu(W/L)$ is the geometric sensitivity parameter with W and L as the width and the length of the channel, respectively, μ is the electron mobility in the channel and C_{ox} is the oxide capacity per unit area.

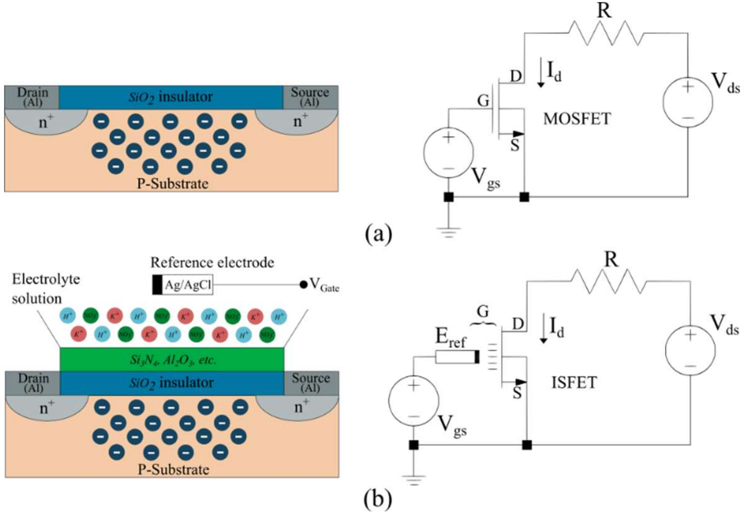

Figure 1. Metal-oxide-semiconductor Field-effect transistor (MOSFET) (a) and Ion-Sensitive Field Effect Transistor (ISFET) analogy (b). G = gate, D = drain, S = source, E_{ref} = reference electrode, V_{ds} = drain-source voltage, I_d = current drain and V_{gs} = gate voltage.

Commonly, in MOSFET devices, I_d is a unique function of the input voltage V_{gs} because β, V_{ds} and V_t (adjusted in factory) are constants. For the ISFET case, the threshold and gate-source voltages are variables in the system. Now, in the term V_t chemical variations are induced, whereas V_{gs} is a DC voltage that directly modifies I_d and is produced by a reference electrode. This influence of chemical variations (or rather ionic activities) is evident in the ISFET voltage threshold, as expressed in equation (2):

$$V_t = E_{ref} - \psi + \chi^{sol} - \frac{\phi_{Si}}{q} - \frac{Q_{ox} + Q_{ss} + Q_B}{C_{ox}} + 2\phi_f \tag{2}$$

The term $(-\phi_{Si}/q) - ((Q_{ox} + Q_{ss} + Q_B)/C_{ox}) + 2\phi_f$ in equation (2) is a little similar to V_t expression in the MOSFET equation, where: ϕ_{Si} is the silicon work function, q is the elementary charge, Q_{ox} is the fixed oxide charge, Q_{ss} is the surface state density at the silicon surface, Q_B is the depletion charge in the silicon and ϕ_f is the Fermi-potential The term $E_{ref} - \psi + \chi^{sol}$ is the only non-constant part of equation (2) given by the potential of the reference electrode E_{ref}, the chemical input parameter ψ and the surface dipole potential of the solvent χ^{sol}. Meanwhile, $\psi + \chi^{sol}$ is the interfacial potential at the solution/oxide interface.

It is possible to analyze the I_d/V_{ds} curves (Figure 2) to understand better the behavior of this sensor. By connecting the ISFET drain, gate, and source terminals to a curve tracer, two scenarios can be proposed. In the first case, it is possible to obtain an I_d family of curves from the variation of V_{gs} and V_{ds} but maintaining the chemical parameter constant through the aqueous substance (Figure 2a). The second case corresponds to obtaining the I_d family of curves from the V_{ds} variation and the change of the chemical parameter from different aqueous solutions but maintaining V_{gs} equals to zero (Figure 2b). In this latter scenario, it is widely accepted to have $V_{gs} = 0$ in the most conventional ISFET readout circuits. To achieve this value, the reference electrode terminal needs to be placed in the circuit common point or ground (GND).

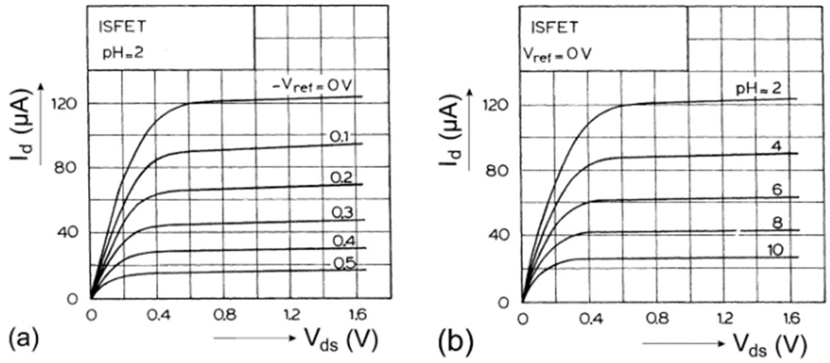

Figure 2. Drain current/ drain-source voltage (I_d/V_{ds})/ curves from curve tracer shown in (a) for pH = 2 constant buffer and in (b) for $V_{gs} = 0$ electrical constant parameter (After Bergveld, 2003).

At the beginning, ISFET was considered as an electronic device to detect hydrogen ions H^+ (pH) in aqueous solutions. For that purpose, Ta_2O_5 membranes are deposited in the floating gate of the ISFET (Wong and White 1988), which is still used today in many cases. Some of ISFET commercial and research devices, and an example of the size of a commercial/research sensor are illustrated in Table 1 and Figure 3, respectively. Later, the ISFET concept was adapted to allow the sensor to detect other types of ions such as potassium or nitrate (Wilson et al. 2001), which converts ISFET into a ChemFET (Chemical Field Effect

Transistor). This device has ion selective feature, which allows the detection of the target ion over other interfering ions by means of an ion sensitive membrane. Some authors claim that the ChemFET approach is empirical rather than theoretical, and pH sensitivities below the theoretical Nernstian value could not be explained (Bergveld 2003). However, other authors stated that the electrochemical cell potential of the sensor can be expressed by the Nikolsky-Eisenman equation.

Table 1. Commercial and research Ion-Sensitive Field Effect Transistor (ISFET) devices with technical characteristics. OEM is original equipment manufacturer, o/r is OEM/research, dnr is does not report, dec is decade, cpp is commercial probe package and ppme is pH pocket Meter

Company	Variable	Range	Accuracy	Sensitivity	Measuring temperature range	Type of probe package	Country
1	pH	2 – 12 pH	0.01 pH	50 mV/pH	0 – 100 °C	o/r	Thailand
2	pH	0 - 14 pH	± 0.01pH	dnr	0 – 80 ºC	o/r	Netherlands
3	pH	1 - 12 pH	0.05 pH	55 mV/pH	0 – 80 ºC	o/r	Switzerland
	K^+	$5\cdot10^{-4}$ - 0.1 M	3 mV	50 (±5) mV/dec	0 – 45 °C		
	Na^+	$1\cdot10^{-4}$ - 0.1 M		50 (±5) mV/dec			
	NO_3^-	$5\cdot10^{-4}$ - 0.1 M		- 48 (±5) mV/dec			
	$H_2PO_4^-$	$1\cdot10^{-3}$ - 1 M		- 38 (±5) mV/dec			
4	pH	1 - 13 pH	± 0.02 pH	52 - 55 mV / pH	dnr	o/r	Spain
	Na^+, K^+, NH_4^+, Ca_2^+, Cl^- and others		dnr				
5	pH	0 to 14 pH	± 0.02 or ± 0.05 pH	-	–15 to 135 °C	cpp	Switzerland
6	pH	2.0 to 12.0 pH	0.1 pH	± 0.1pH	5°C to 40°C	ppme	USA
7	pH	0 - 14 pH	dnr	dnr	–10 to 110 °C	cpp	USA
8	pH	0 - 14 pH	0.1 or 0.01pH	dnr	0 to 60ºC	cpp	USA
9	pH	0 - 14 pH	dnr	dnr	0 to 60ºC	cpp	Japan
10	pH	0 - 14 pH	dnr	dnr	0 to 80ºC	cpp	Switzerland

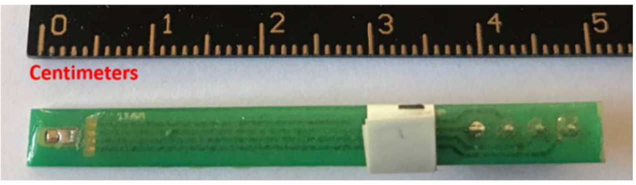

Figure 3. Actual size (in cm) of an Ion-Sensitive Field Effect Transistor (ISFET) sensor. The measurement area of the sensor corresponds to 0.1cm^2 approximately.

2.2. ISFET types for bio-sensing applications

Based on different structures and membranes, the use of these sensors have been expanded to various fields of science, engineering and research, including industrial, environmental and biomedical applications. According to Kaisti (2017), ISFET can be used to detect chemical compounds in different kinds of samples. Measurement begins with preparing the sample extraction. Then, the extraction is put in direct contact with the membrane, which leads to generating current changes (commonly denoted by I_d [Eqn. 1]). Finally, the signal obtained from the transduction goes through a readout circuit, where electronic compensations are made (in analog or digital way), and the result is digitized, and the processed signal is displayed to the end-users.

Several types of ISFET exist according to the application. These include the ISFET/Reference field-effect transistor (REFET), the Chemically Sensitive Field-Effect Transistor (ChemFET), and the Enzyme Field-Effect Transistor (ENFET). REFET is a pair-matched array between a conventional ISFET and identical FET (Bergveld, 2003; Khanna et al., 2009; Zabrowski et al., 2014). The array uses a metal wire (like platinum) for grounding the sample solution (reference electrode into solution and wiring to GND circuit reference) and applying a differential measurement between the ISFET and FET to detect the ion concentration in a chemical solution. The main advantage of REFET is the capability to suppress the common-mode-rejection-ratio (CMRR) in the sensor signal. ChemFET is considered an ISFET sensor because it retains the same characteristics as an ISFET (Bergveld, 2003). Unlike the ISFET sensor, additional membranes are deposited in the ChemFET, which allows detecting different types of ions in aqueous solutions. The ENFET (enzyme FET) has an enzyme layer, which forms part of the entire insulator layer in the FET structure (Dzyadevych et al., 2006). Multiple authors have reported the use of ENFETs to detect cholesterol (Ishige et al., 2009), glucose (Yao et al., 2007), and Urea (Temple-Boyer et al., 2008). In addition to the above ISFET types, there are subcategories of these sensors such as unmodified CMOS ISFETs, FET sensor Floating-Gate, Extended-Gate FET sensor and Dual-Gate FET sensor (Kaisti et al., 2017).

ISFETs, ChemFETs and ENFETs are considered Bio Field-Effect Transistors (BioFETs). However, there are other BioFETs having different FET architectures, e.g., Bottom-Gate FETs, Electrolyte-Gated FETs (EG-FET), and Electrochemical Transistors (ECT) (Elli, 2022). Some examples of these BioFETs are the Carbon Nanotubes Field-Effect Transistors (CNTFETs), the Electrolyte-Gated Organic Field-Effect Transistor (EGOFET), and the Enzymatic biosensors having organic electrochemical transistors (OECTs). The latter was reported for the detection of pesticides e.g., atrazine in seawater and riverine water (Belkhamssa et al., 2016), viruses e.g., Plum Pox in fruit trees (Berto et al., 2019) and glucose and sucrose in trees (Diacci, 2021). Even FET sensors based on Silver/Graphene composites fabricated using Nozzle-Jet-Printed technology was reported for the measurement of phosphate concentrations in lake waters (Bhat et al., 2019). While these BioFETs are widely reported in environmental applications, the potential of these devices needs to be harnessed in the next decade for the measurement of soil chemical parameters for Digital Agriculture applications.

2.3. ISFET for soil chemical parameters measurement

Commonly, when referring to in-situ and/or on-the-go measurements of soil chemical parameters for PA applications, spectroscopy-based and electrochemical sensors are the most common PSS technologies (Burton et al., 2020; Kuang et al., 2012). Among the spectroscopy methods, Visible and Near Infrared (vis-NIR) spectroscopy (Morellos et al., 2016), mid infrared red (MIR) spectroscopy (Afriyie et al., 2021), X-Ray Fluorescence (XRF) (Tavares et al., 2020) and Laser-Induced Breakdown Spectroscopy (LIBS) (Erler et al., 2020) are the most commonly used. These spectroscopy techniques are reported frequently for successful measurement of total nutrient contents, micronutrients, and pH. Individual use or the fusion of these spectroscopy techniques enable successful estimation of organic matter (Kuang et al., 2012; Liu et al., 2021), organic carbon (Javadi et al., 2021) and lime buffer capacity (Ji et al., 2019) in soils. However, none of them has been successfully used for the measurement of mineral nitrogen for example. In addition, spectroscopy based-sensors (e.g., vis-NIR, XRF and LIBS) are usually expensive and require extensive calibration methods to obtain correct estimates of the chemical parameters. They are sensitive to moisture content, which affect the accuracy of measurement and limit their use for in situ applications. Furthermore, there is need for extra soil sample preparation to enable successful scanning with the LIBS, which is also true to a given extent for the XRF. Although the effect on soil moisture content on the accuracy of these spectroscopy techniques can be removed, by spectra pretreatment and advanced modelling methods (Mouazen et al., 2020; Nawar et al., 2020; de Santana et al., 2019), the extra effort of sample preparation, especially for LIBS, makes it not suitable for in situ applications currently.

The most common electrochemical sensors in PSS correspond to ISE and ISFET, which are capable of measuring pH and available nutrients. These sensors cannot estimate total nutrients as spectroscopy-based sensors do. Their sensitivity to specific ions such as nitrate (Chen et al., 2020) or phosphate (Hinck et al., 2018) allows for more detailed inferences regarding soil fertility. Moreover, other sensing technologies based on electrochemical or biosensing devices have demonstrated their ability to measure chemical properties in soils. For example, cantilever-based biosensors (Patkar et al., 2017), electrophoresis-based microfluidic biosensors (Smolka et al., 2017; Xu et al., 2017) and multi-target capacitive microneedle sensors (Mugo et al., 2022) are devices capable to quantify nitrate, phosphate and in some cases, pH. Even qualitative methods with the capability of differentiating soil nutrients such as N, P, K, Ca, and Mg can be implemented using microfluidics electronic tongues based on gold-interdigitated electrodes (Braunger et al., 2017). Other technologies like Carbon-Based Screen-Printed Electrodes (Singh et al., 2020) or epoxy resin nanocomposite film-based conductometric microsensors (Patil et al., 2019) are suitable for pH quantification in soil solutions.

Each electrochemical sensor has its characteristics. Solid-state ISE sensors have a long life, their excitation circuits are not complicated, and they have a wide range of membranes for the detection of several available nutrients. Some works even show miniature ISE devices to be successfully used for soil ion determination using screen-printed methods (Ali et al., 2019; Dam and Zevenbergen, 2019; Rosenberg et al., 2018; Ruane and Sonnino, 2010). However, response and stabilization times are usually higher than 20 seconds (Sentek, 2018), and their prices can be high. ISFET sensors are relatively cheaper, of a smaller size and allow easy integration of multiparametric probes. Their response times are of less than 6 seconds, which make them more suitable for PA applications. Nevertheless, their electronics are usually more complicated. Still, with reliable results, their lifetime is shorter compared to ISE, and they are highly sensitive to electrostatic discharges, which commonly occur when an expert in the field does not handle the sensor properly.

2.4. ISFET source of errors

Like any measurement instrument, an error is expected from ISFET sensors and manufacturers used to provide indication of the error. For example, a pH ISFET manufactured by the company 3 (Table 1) has an error of ±0.02, meaning that the error of measurement of pH = 6.52 may range between 6.50 and 6.54. In practice, factors affecting measurement errors are mainly associated with the sensor calibration, offsets in the electronic instrumentation (readout circuit), and the non-idealities. Errors in the sensor calibration are attributed to human error and laboratory instrumentation e.g., including the glassware, balance for weighing reagents, as well as the quality of the water used to prepare the calibration solutions. The electronic instrumentation circuitry can also bias the signal, hence, induce errors. In these circuits, offset in amplifiers and tolerances of passive elements (capacitors, resistors, etc.) are the primary source of errors. Other errors are associated with the ISFET non-idealities (temperature, drift, and noise). Calibration errors can be reduced by using quality reagents and water, and quality laboratory instrumentations (Gao and Lloyd, 2020). Errors associated with electronic instrumentation can be overcome by understanding the characteristics of the electronic components (passive and active) and by including offset and gain calibration circuits (Guerrero et al., 2013). Regarding the non-idealities of the ISFET sensor, these can be mitigated by physical modification of the device or by using specialized readout circuits, as specified in section 3.1 of this paper.

3. Towards ISFET implementation in Precision Agriculture

Compared to the biomedical sector, the use of ISFET in agriculture is limited particularly for soil measurement in PA applications. However, isolated cases of pH and available nutrients detection in soils have been reported in literature. The following section shows these cases for different application modes.

3.1. On-The-Go proximal soil sensing platforms

On-the-go proximal soil sensing platforms may integrate one or more sensors for sensing several variables, with the aim of mapping the spatial variability in soil characteristics. These platforms (Figure 4) are attached to a moving vehicle such as quadbikes, or tractors, and data are collected on-the-go (Mouazen 2006; Veris Technologies 2018). Different sensor technologies, e.g., mechanical, spectral, electrical, gamma-ray or electrochemical techniques, are used for the collection of geographically referenced data of several attributes at high spatial resolutions. These automated sensing platforms enable high density readings (+500 reading per ha), quickly and at a relatively low-cost (Adsett et al., 1999; Adamchuk et al., 2004; Viscarra Rossel and Walter, 2004).

Figure 4. On-The-Go multisensory soil-sensing platform from Precision Soil and Crop Engineering group at Ghent University. This platform includes visible and near-infrared, gamma-ray, depth, and electrochemical sensors, as well as an RTK-GPS system among other devices.

On-site rapid soil nutrients measurement is the ideal approach for implementing PA. In the late 1990s Adsett et al. (1999) have reported an on-the-go platform for the measurement of soil nitrate, using a custom-built soil sampler and a commercially available ISE. With a prediction time of 6 seconds and using a 1.43 scaling factor, the platform achieved an $R^2 = 0.99$. Adamchuk et al. (1999) developed an automated On-the-Go system for soil pH measurement, achieving $R^2 = 0.83$ and a standard error of prediction of 0.45. The system consisted of a sampling mechanism, compressed air and rinsing water providing units, an ISE pH sensor, a GPS receiver, and a notebook computer. The innovation was the sampling mechanism since soil samples can be placed in contact with the ISE (direct soil measurement) through a defined location and depth. This on-the-go measurement system has found its way to market by Veris® Mobile Sensor Platform (MSP). Lund et al. (2004) evaluated the performance of an ISE electrode of the MSP system to map soil pH, obtaining of $R^2 = 0.95$ in moist soils, and $R^2 = 0.84$ in dry soils. The accuracy was improved by allowing for 40% additional time. The system was later integrated with a soil resistivity sensor to measure electrical conductivity (EC) and a NIRS sensor to measure organic carbon. Adamchuck et al. (2007) used the MSP system to map soil pH ($R^2 = 0.81$), highlighting the potential for successful variable rate liming. Similarly, Schirrmann et al. (2011) used the MSP system to measure map soil pH in three different fields, reporting R^2 values of 0.71, 0.63, and 0.84 for sand/silty sand, silty sand, and loam/silty sand soils, respectively. It was concluded that it is more accurate to calibrate ISE with $CaCl_2$, because differences in soil pH of 0.1 units can lead to considerable differences in lime recommendations. Sethuramasamyraja et al. (2008) evaluated an agitated soil measurement (ASM) method for soil pH, soluble potassium, and residual nitrate using an ISE. They immersed an ISE sensor into a stirred (agitated) 1:1 soil:water suspension made with deionized water using an integrated Agitation Chamber Module (IACM) attachment to the MSP system. They achieved R^2 values of 0.85 – 0.89 for pH, 0.50 – 0.54 for K, and 0.14 – 0.32 for nitrate. Sibley et al. (2009) suggested that the use of nitrate ISE sensors allow the generation of soil nitrate maps using of nitrate extraction and measurement sub-units (NEMS). In this work, a NEMS was mounted on a tractor for On-the-Go field measurement, reporting $R^2 > 0.9$.

Lobsey et al., (2010) developed and evaluated a multi-ion measuring system of soil nitrate, potassium and sodium using ISE sensors. The system provided a fully autonomous sample analysis, including reagent injection, agitation, and kinetics monitoring and soil nutrient predictions with an R^2 of 0.92 for nitrate, 0.99 for sodium, and 0.99 for potassium, using 30s analysis time. Schirrmann et al. (2011) implemented an ISE on-the-go sensing platform to measure and map pH, and available P, K, and Mg, reporting R^2 values of 0.92, 0.91, 0.73 and 0.75, respectively. Tsukor et al. (2019) developed an automated mobile field laboratory for on-the-go nitrate, phosphate, and potassium , analysis using ISFET sensors, obtaining a sensitivity of around 58 mV/ion. Despite the several above-listed studies on On-the-Go sensing platforms for soil nutrients and pH, there are essential challenges hindering the development of commercialized versions (except the Veris pH sensor). These include the time needed for extraction preparation and analysis, complicated and delicate mechatronics requirement, multi-source noise, and achievable level of accuracy. The majority of the on-the-go sensing platforms using electrochemical technologies adopted ISE, while very minor works on the use of ISFET were reported. This necessitates future research to explore further the potential of ISFET for on-the-go sensing, capitalizing on its advantageous compared to the ISE technology.

3.2. Laboratory and stationary field sensors

The challenges of the use of electrochemical sensors for laboratory and stationary field sensing, are less extreme, compared to those encountered with the On-the-Go systems. Some researchers have developed and tested prototypes to measure soil nutrient and pH, whose accuracy and precision are validated under different laboratory and field conditions and experiments.

Artigas et al. (2001) conducted several laboratory experiments using different ISFETs to analyze loam soils extracts. Results obtained with ISFETs and standard methods showed t-paired test values of 3.16, 1.95, 0.85 and 5.14 for calcium, potassium nitrate and pH, respectively. Viscarra Rossel and Walter (2004) attempted to determine the required times for rapid and accurate field-based measurements of soil pH, using an ISFET sensor and a four steps protocol: soil drill, water addition, ISFET insertion in the soil and pH measuring. The protocol and soil samples collection (for conventional lab analysis) were performed in a field near Rennes, France. Further analysis showed that the accuracy of ISFET measurements (using a soil measuring time of 10 seconds) versus lab analysis was 0.34 pH units. Kim et al. (2007) reported laboratory evaluation of a sensor array including three different ISEs for the simultaneous determination of nitrate , available K, and available P in soil extracts. Thirty-seven Illinois and Missouri soils were used in the experiment, and these were subjected to the Kelowna soil extractant (0.25 mol/L CH_3COOH + 0.015 mol/L NH_4F). Results showed that the ISEs provided good accuracy compared to values obtained with standard laboratory methods ($R^2 = 0.89$, $P < 0.001$), ($R^2 = 0.85$, $P < 0.001$) and ($R^2 = 0.81$, $P < 0.001$) for nitrate , potassium and phosphate, respectively. Later, Birrell and Hummel (2001) developed an integrated multi-sensor soil analysis system, for which ISFET technology was coupled with flow injection analysis (FIA) to produce a real-time soil analysis system with automatic sample extraction. The system enabled achieving an $R^2 > 0.9$ for soil nitrate measurement in manually extracted soil solutions, which required 1.25 seconds per sample and an appropriate calibration solution (multiple points of $NaNO_3$ in a 0.01M $CuSO_4$ solution). Similarly, Lehmann and Grisel (2014) presented a multi-sensor probe that has four ISFET sensing elements for real-time soil nutrients monitoring of potassium, nitrate, phosphate and pH. The multi-sensor probe was validated under calibration solutions and results revealed that its sensitivity with the different ions was -55mV/decade for pH, 48mV/decade for potassium and -33mV/decade for nitrate.

Other studies demonstrated the ability of ISFET sensors to make direct measurements in the soil, without the need to prepare a soil extract. Joly et al. (2022) conducted a laboratory experiment in which ISFETs were buried in clay-silt soils having, moisture contents between 40% and 100%, to detect ammonium and nitrate changes. The sensor exhibited good detection performance over a period of six months with sensitivities around 56 mV/decade. Hong et al. (2022) developed a multiparameter probe to measure soil pH, water content (SWC), electrical conductivity, and temperature, under laboratory conditions. Authors reported accurate pH measurement when the SWC was above 16.3%. All the above studies were laboratory based, hence, future work should move towards field experiments, to test the performance of these sensors for "real-time" stationary measurement of soil nutrients.

In short, the use of stationary field sensors is becoming fundamental for research studies or inventory tasks, during which in-depth understanding of the sensor performance, and issues related with application in the practice are necessary. To fulfill this, it is required to integrate these sensors in Wireless Sensor Networks (WSN's), composed by many nodes distributed, for example, over an area of a field. Each node enables the measurement of soil properties using ISFET sensors while the other sensors can measure other properties e.g., moisture, temperature, and gases. The nodes should be of ultra-low-cost, low-energy consumption, and small size. In addition, the WSN should not interfere with fieldworks. Advances in nanomaterials and sustainable energy should be used for fast deployment of these WSN's.

4. Electrical performance and non-idealities of ISFET sensors

4.1. Sensor electrical performance

When in operation an ISFET sensor may well be affected by different ambient conditions including the analyte moisture (e.g., from soil extract), temperature (including both ambient and analyte), atmospheric pressure, luminosity (natural or artificial), and the standard electrostatic discharge (ESD). Except the soil:water ratio (for a sensor within a useable lifetime), all these variables can affect the output voltage (e.g., mV/pH) because they influence the drain current (I_d). Meanwhile, the ESD effect is related to the sensor performance deterioration under certain operating conditions.

4.1.1. ISFET operating temperature

During measurement, ISFET sensors are affected by the ambient temperature, and the temperature of the analyte (soil extract) being measured. In most cases, manufacturers of ISFET sensors, set the nominal operating temperature, in the range from 0°C to 80°C, which is not questionable since it is part of the ISFET materials. Nevertheless, the drain current I_d or the voltage temperature dependence of the readout circuit output is clearly affected by ambient temperature. This temperature effect is part of the non-idealities of the ISFET sensor. Figure 5 shows several output voltage behaviors influenced by temperature (8.04 mV/pH) by an ISFET sensor with Si_3N_4 gate type (Chung et al., 2006).

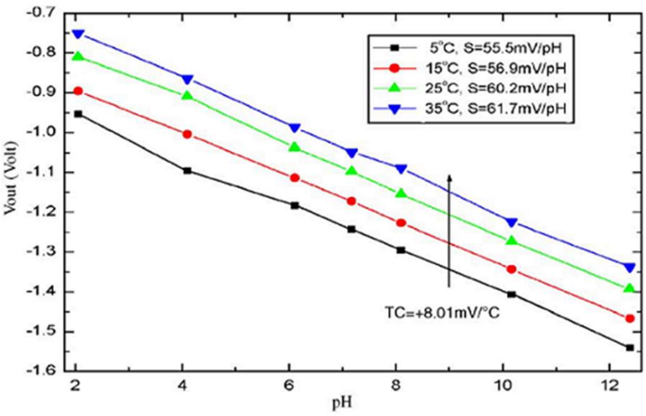

Figure 5. Temperature performance Si_3N_4 gate Ion-Sensitive Field Effect Transistor (ISFET) response for different pH at various temperatures (After: Chung et al., 2006)

4.1.2. Analyte moisture effect on ISFET sensor performance

The effect of the analyte moisture is not relevant in the case of ISFET sensors. This also applies for the direct measurement mode by immersing a sensor directly in wet soils. Gràcia et al. (1992) immersed an ISFET sensor into an electrolyte for three months at approximately 25°C, to study the effect of moisture on a passivating SiO_2 membrane, finding negligible effect, as no changes were observed in the measured current values.

4.1.3. Effect of atmospheric pressure on ISFET sensor performance

Another but not important effect on performance of ISFET sensors is that of the atmospheric pressure. Le Bris and Birot (1997) showed a maximum change in registered sensor reading of 1 mV when subjected to a pressure range from 0 to 3 MPa for 43 h. They also found insignificant effect on sensitivity of an ISFET sensor under artificially applied pressure (Table 2). Other authors emphasize that the channel insulator and substrate, having a solid-state FET, are intrinsically insensitive to pressure. These characteristics (along with others) make the ISFET an excellent candidate for robotic floats/gliders, Autonomous Underwater Vehicles (AUVs), and Remotely Operated Vehicles (ROVs) applications (Martz et al., 2010).

Table 2: Variation of Ion-Sensitive Field-Effect Transistor ISFET slope values at different pressure conditions and exposure time (After Le Bris and Birot 1997)

Time	**Pressure (Mpa)**	**Slope (mV/pH)**	**Time**	**Pressure (MPa)**	**Slope (mV/pH)**
0	Ambient atmosphere	43.5	7 h	3	44.8
70min	1	44.0	22 h + 45 min	3	44.3
90min	1.5	44.2	22 h	3	44.6
105min	2	44.3	31 h	3	44.3
210min	3	44.2	46 h + 45 min	3	44.6

4.1.4. Light exposure effect on ISFET sensor performance

Light affects the performance of ISFET, due its effect on the sensor membrane. Ito (2000) showed that exposures to fluorescent light strongly influence long-term sensor stability, and drifts of ISFET are accelerated under intensities larger than 1000 lux. Examining the performance of several ISFETs having Ta_2O_5 gates exposed for on-off periods of fluorescent light for 7h, Baldi et al. (2001) observed noticeable increases in drift during the "on" periods (curves a and a' in Figure 6a). However, adding a special additive to the Ta_2O_5 ISFET gate, small changes in drift can be seen when the sensor is exposed to fluorescent light (curve b).

4.1.5. Electrostatic discharge effect on ISFET sensor performance

ISFET sensors are highly sensitive to Electrostatic Discharge (ESD) when submerged into aqueous solutions or connected to a measuring tool that is not isolated from the ground, or when the operator handles these sensors without any anti-static protection. One of the most critical effects caused by ESD is the threshold voltage shift. To prevent the ESD effect it is necessary for the operators to use static control measures like grounding wrist straps. Baldi et al. (2001) introduced, under experimental conditions a high electrostatic discharge of 1.2kV in an ISFET sensor, which could occur (during a short time) only if the sensor is handled without ground protection. As a result, the V_{gs}/I_d characteristic curve of the ISFET suffers a 15V displacement of the initial voltage (Figure 6b), changing the device's behavior.

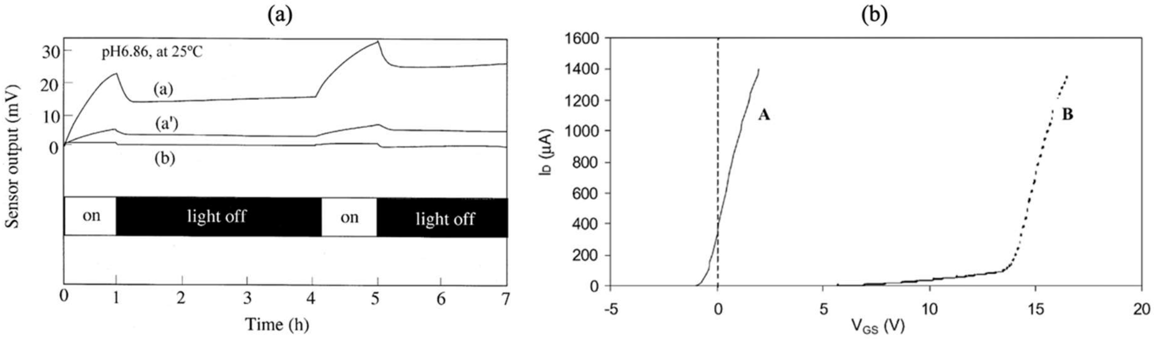

Figure 6. Light and pressure performance for an Ion-Sensitive Field Effect Transistor (ISFET) sensor. (a) Base line drifts of Ta_2O_5 ISFET gate under the light switching test and the effect of light intensity (After Ito, 2000). (b) Gate characteristic of an ISFET before (A) and after (B) receiving a 1.2 kV electrostatic discharge (ESD) (After: Baldi et al., 2001).

4.2. Non-idealities of ISFET sensors

Several non-idealities were reported in the literature to affect the ISFET sensors. These are discussed below.

4.2.1. Trapped charge

It corresponds to the formation of holes in the ISFET transistor, which is usually associated with oxygen vacancies in the SiO_2 layer that leads the charge to be trapped together with the oxide. Consequently, a displacement in the ISFET threshold voltage and channel mobility degradation take place (Milgrew and Cumming, 2008).

4.2.2. Drift

Jamasb (2004) defined drift as a "... relatively slow, unidirectional temporal variation in the threshold voltage and, hence, in the drain current of FET in the absence of changes in the measurand of interest". For instance, in an ISFET with Si_3N_4 gate, the drift effect is associated with a relatively slow conversion of the silicon nitride surface into a hydrated SiO_2 surface or an oxynitride layer (Chen and Chan, 2008). Other authors reported that drift depends on several factors, including pH of the solution, the surface material, and the device ISFET FET structure size (Sohbati and Toumazou, 2015).

4.2.3. Temperature

Temperature is one of the ambient variables that affect most the output response of ISFET devices, and lead to a nonlinear behavior (Chan and Chen, 2007). The thermal agitation directly affects the flow of electrons, as of ISFET devices are made based on the MOSFET technology (Chou et al., 2000). On the other hand, temperature variations of ionic solutions tend to generate a deviation in the drain of ISFET current (Chin et al., 2001). In addition, the output response of the sensor can be affected by a given temperature range. Chung et al. (2006) observed an increase in the output voltage of 8.01 mV/°C of an ISFET pH sensor subjected to a temperature increase from 5° to 35°C (Figure 5). Since several manufacturers do not provide this data, it becomes necessary to characterize the mV/°C behavior by the users.

4.2.4. Electrical Noise

Although very few studies evaluated the ISFET noise, some authors attempted to understand how noise occurs. Noise can be generated by the FET structure of an ISFET, the chemical interface (e.g., analyte or ionic solution), and the polymer membrane at the ISFET gate., and the polymer membrane in the ISFET gate. Moser et al. (2016) emphasized that the influence of chemical noise over electric noise is steadily dependent on the technology to be implemented. Also, Das et al., (2015) found an equivalent model for the electrode-electrolyte-FET structure on the ISFET sensor noise. The model consisted of five sources of noise generation e.g., a white noise source at the electrode-electrolyte junction, two noise sources (white and 1/f) at the electrolyte bulk, and two noise sources (white and 1/f) at the FET structure. The analysis and understanding of ISFET noise is essential to improve the quality of data collected and accuracy of the system overall.

5. ISFET electronic instrumentation

The most important task during the development or integration of ISEFET-based measurement systems is to collect accurate signals. Therefore, it is necessary to use instrumentation circuits to ensure the sensor biasing (fixed voltages, currents, or both in the ISFET), which allows for acquiring electrical signals related to the ions concentration in an analyte. In the context of ISFET sensors, instrumentation circuits can be referred as analog readout circuits (sometimes called front-end stages) and can be designed in two ways. The first corresponds to the Complementary Metal-Oxide-Semiconductor, commonly adopted for complex biomedical applications, for which it is convenient to integrate readout circuits and hundreds of ISFET sensors in a monolithic way, that is, in a single substrate. The use of lab-on-a-pill miniaturized devices for measurements in the intestinal tract (Cumming, 2011) can be mentioned as an example. The second type concerns the development of discrete electronic circuits, integrating discrete components e.g., transistors, operational amplifiers, resistors, capacitors, etc., printable circuit boards (PCB). For agricultural applications, the discrete electronic readout is the most convenient circuit at present, given its design and manufacture simplicity and versatility of integration. Simplicity is associated with free electronic design automation tools offered by the ecosystem, the non-use of "super-specialized" human capital with CMOS knowledge for hardware design, and the broad portfolio of discrete electronics provided by the market. The manufacturing process should ensure the development of rapid prototypes using homemade elements (e.g., laser printer, toner transfer paper, copper-clad laminate, and Iron (III) chloride for cooper etching) or those available in the market (e.g., PCBWay, JLPCB or 4PCB). The versatility of integration is associated by their capacity to adjust on the fly and repeat failed processes at low cost (in comparison with CMOS processes) when used for PA applications. The readout circuits can be classified as performing single-ended or differential measurements. Each measurement type has its different readout circuits, advantages, and disadvantages, which are presented below. It is also possible to classify the measurements made with these circuits as amperometric or potentiometric (Dei et al., 2019). This classification is used in the context of electrochemical sensors but is not common in ISFET sensors.

5.1. Single-ended measurement circuits

Readout circuits that use single-ended measurements are composed of only one ISFET device. A commonly used topology within these circuits is the source and drain follower. Different types of these circuits are showed in Figure 7(i-iii). Within these circuits, an ISFET is polarized in a linear region with constant drain-source voltage and drain current values. Once this polarization is achieved, signals inversely proportional to the channel resistance of the device in the linear region are obtained, which express the target ion's behavior in the solution.

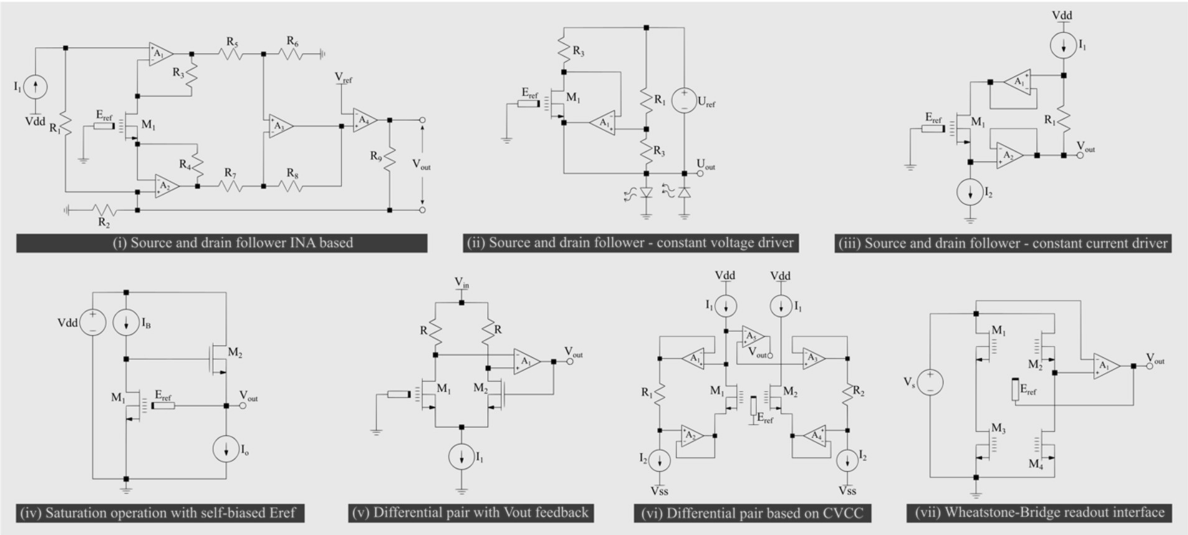
(i) Source and drain follower INA based

(ii) Source and drain follower - constant voltage driver

(iii) Source and drain follower - constant current driver

(iv) Saturation operation with self-biased Eref

(v) Differential pair with Vout feedback

(vi) Differential pair based on CVCC

(vii) Wheatstone-Bridge readout interface

Figure 7. Single-ended measurements (i-iii) and differential measurements (iv-vii) readout circuits. The first three circuits are realizations of the classic source and drain follower: (i) Based on an instrumentation amplifier (INA), (ii) with a constant voltage driver and (iii) using a constant current driver. The following circuits are: (iv) saturation-based Ion-Sensitive Field Effect Transistor (ISFET) readout circuit, (v) differential amplifier, (vi) differential pair based on constant voltage constant current circuit (CVCC) and Wheatstone-bridge readout interface.

5.1.1. Source and drain follower based on INA

This configuration use of an instrumentation amplifier (INA) composed of four operational amplifiers (OPAMPs) (A_1- A_4). Figure 7(i) shows the connection of an ISFET sensor through inverter terminals of the OPAMPs A_1 and A_2. These OPAMPs, having a low resistance, offer, on the one hand, the possibility of positioning the sensor and the readout circuit through long cables and, on the other hand, being insensitive to interference from external electric fields and static charges (Bergveld, 1981). In the circuit, the reference electrode is connected to a GND, the constant voltage V_{ds} is obtained from $I_l \cdot R_l$, and the current I_d is fixed by the feedback current from the instrumentation amplifier (INA) output. Finally, the circuit's output signal (V_{out}) is determined by the ISFET threshold voltage (V_{th}) times an amplification factor (R_9/R_2). According to (Morgenshtein, 2003), this can be expressed mathematically as:

$$V_{out} = \Delta V_{th}\left(\frac{R_9}{R_2}\right) \tag{3}$$

5.1.2. Source and drain follower with constant voltage driver

This "source and drain follower" is characterized by the ease of fixing the linear region in the sensor through a voltage source (U_{ref}) and several resistors. In the circuit of Figure 7(ii), once the values for $V_{ds} = U_{R3}$ and $I_{ds} = U_{ref}/R_3$ are adjusted, V_{gs} is kept constant by automatically adapting the source potential to GND and changing the threshold voltage V_t of the ISFET (Bergveld, 2003).

5.1.3. Source and drain follower using a constant current driver

One of the preferred alternatives for the integration of ISFET sensors in discrete applications, is this source and drain follower that employs constant current sources. Figure 7(iii) illustrates how the voltage V_{ds} is produced by $I_l \cdot R_l$ and the current $I_{ds} = I_l \ \forall \ I_2 = 2I_l$ (Milgrew and Cumming, 2008; Morgenshtein, 2003). By establishment of robust and constant current sources, such as the cascode current mirror, it is possible to achieve precision and stability in the I_{ds} and V_{ds} values, which represents a great advantage for measurements. According to Morgenshtein (2003), the output of this circuit can be written as follows:

$$V_{out} = -V_{th}(\mathrm{ISFET}) - \frac{I_2}{\beta I_1 R_1} - \frac{I_1 R_1}{2} \tag{4}$$

5.1.4. Saturation-based ISFET readout circuit

Unlike the previous 3 single-ended circuits, the saturation-based circuit is not based on a source-voltage follower. Thus, to obtain threshold voltages proportional to concentration changes in the electrolyte, the ISFET sensor is polarized in the saturation region. Figure 7(iv) shows the design of Chan and Chen (2007), which evidences an ISFET device operating in the saturation region through the constant current source I_B and a source follower formed by the M_1 transistor and the Io current source. This is to obtain an output signal from the reference electrode, which can be written as:

$$V_{out} = V_{gs} = V_{th(ISFET)} + \sqrt{\frac{2I_B}{\mu_N C_{OX}(\frac{W}{L})}} + I_B R_S \tag{5}$$

5.2. Differential measurements circuits

A pair or multiple pairs of ISFET, and even a pair formed between an ISFET and a MOSFET, are used in readout circuits to improve differential measurements. The main feature of this configuration is the ability to cancel the common-mode voltage between both sensors, allowing the attenuation of effects of temperature, noise and drift. Some of these circuits are shown in Figure 7(v-vii).

5.2.1. Differential amplifier circuit with feedback

To attenuate the undesired effects of temperature (Bergveld, 1981), the circuit in Figure 7(v) proposes the use of a differential amplifier with output voltage feedback V_{out} to the gate of the MOSFET M_2. The circuit maintains a constant ISFET drain current and compensates for its temperature sensitivity. This occurs because thermally induced changes in the ISFET and MOSFET drainage currents are rejected due to the common mode that occurs in the differential amplifier configuration (Morgenshtein, 2003).

5.2.2. Differential pair based on constant voltage constant current circuit

The first definition of this circuit as introduced by Palán et al. (1999). It is based on the attenuation of multiple non-ideality, namely, temperature dependence, common-mode noise, instability caused by the

ISFET membrane layers and the unstable reference electrode potential problem. This attenuation is achieved by a differential signal, obtained from two ISFET sensors, each in a source-drain follower circuit. Other circuit topologies obtain the differential signal from two ISFET using an INA (Milgrew et al., 2004). The left side of the circuit in Figure (7vi) shows the first source-drain follower with a constant V_{ds} for the ISFET M_1 produced by $I_2 \cdot R_1$, and a constant current I_{ds} given by I_1. The same happens with the right side, that is, constant V_{ds} with $I_2 \cdot R_2$ and constant current I_{ds} through I_1. The signal produced by the ISFET M_1 circuit is directly proportional to the changes of the ion concentration in the electrolyte to be measured, which is translated into changes in the device's threshold voltage. However, the ISFET M_2 is usually non-sensitive to the analyte (e.g., REFET) and its threshold voltage remains the same when there are changes in ion concentrations in the electrolyte. The input expression to the instrumentation amplifier (inverting or non-inverting input), considering both ISFET in the non-saturation region, is given by the following equation:

$$V_{out} = V_{gs} = V_{th(ISFET)} + \sqrt{\frac{2I_B}{\mu_N C_{OX}(\frac{W}{L})}} + I_B R_S \tag{6}$$

5.2.3. Wheatstone-bridge readout interface

Another novel differential circuit is the one proposed in (Morgenshtein et al., 2004a) and (Morgenshtein et al., 2004b) that include a ISFET sensor in a classic Wheatstone bridge. In the circuit of Figure 7(vii), the differential input signal comes from the difference of the threshold voltage of the ISFET's M_1-M_2 and REFET's M_3-M_4 devices. This difference is related to the ion concentration in the electrolyte. The Wheatstone bridge configuration uses a reference electrode common to the ISFET-REFET pairs and is connected to the OPAMP A_1 output in direct feedback mode. This circuit provides high immunity to noise.

5.3. ISFET non-idealities attenuation methods

So far, previous readout circuits have shown the ability to set voltages and currents in an ISFET sensor, which allows fixing a particular operating mode to obtain an output signal proportional to the changes in the ions concentration to be measured. However, due to sensor non-idealities, it is necessary to mitigate their effects, by means of sensor adaptation or compensation with circuits. The former is related to physical intervention of the sensor design, or to coupling of external elements (passive or active) to modify its DC behavior. For example, ISFET pixels can be exposed to ultraviolet light to excite trapped charges in polysilicon gates (Milgrew and Cumming, 2008) and capacitively couple their terminals to minimize the effects of trapped charge that appear during ISFETs manufactured using commercial CMOS technologies (Yan et al., 2009). Regarding the drift attenuation, the restart of the vertical and horizontal electric fields present in ISFET (Welch et al., 2013) is a good alternative at the system compensation level.

Two other non-idealities that should be treated for system compensation are temperature and noise. For the former the aim is to ensure insensitivity to temperature. Chen and Chan (2008) used a readout circuit to fix the sensor in the non-saturation region to dynamically polarizes it in its thermal point. An algorithm enabled external processing of data was used to achieve temperature insensitivity. Other modern approaches use readout circuits that polarize the ISFET in its inverse region to overcome the temperature dependence (He et al., 2020; Sohbati and Toumazou, 2014). Noise in turn is usually compensated by using low-pass filters (Carrillo-Martínez et al., 2016; Chung et al., 2004) as far as ISFET adaptation is concerned.

For the system compensation, signals from the readout circuit are collected, often without modifying their polarization parameters, and these are subjected to digital processing to compensate for the sensor non-idealities. Some configurations may not require digital signal processing, as in the case of differential readout circuits, which are usually used to compensate for drift, noise and temperature non-idealities (Kalofonou and Toumazou, 2014; Milgrew et al., 2004). There are also outstanding circuits for system compensation such as those based on the correlated double sampling (CDS) technique. This discrete-time technique, using switching capacitors, achieves a phase holding to perform arithmetic operations between past and present values, contributing to solving low-frequency signal errors such as drift and 1/f noise (Huang et al., 2015; Premanode et al., 2007).

6. ISFET behavioral modeling

Modeling and simulation allow in depth understanding of the dynamic behaviors of different devices. During the 90s and 2000s, the development of ISFET physical-chemical models took place using semiconductor-based device simulation programs like Simulation Program with Integrated Circuit Emphasis (SPICE). Martinoia et al. (2005) emphasized that to simulate the behavior of ISFETs, two kinds of models should be targeted. The first one is a built-in sophisticated physical-chemical model requiring a hard code built using a software like BIOSPICE. The second one is a macromodel, which is a user-friendly behavioral model, and it can be used in conjunction with the most commercially available SPICE versions.

6.1. ISFET macromodel

The ISFET macromodel (Martinoia and Massobrio, 2000) shown in Figure 8(a) enables the simulation of the ISFET behavior, without encountering the demerit of the built-in model (Martinoia et al., 2005). Several authors have used this model as a reference for their simulation works (Abu Samah et al., 2016; Fernandes et al., 2012; Roziah Jarmin et al., 2010; Sinha et al., 2014). The macromodel also operates under a subthreshold region, which is a useful operating mode when ISFET-based applications require low-power and low-voltage working conditions. The concept consists of two fully uncoupled stages, namely, electrochemical, and electronic stages. Basically, in the electrochemical phase, a signal proportional to the pH changes is generated. This signal is an input for the MOSFET gate (in the model) that makes up the electronic stage.

As seen in the macromodel of Figure 8(a), the parameters E_{ref} (reference electrode), C_{Gouy} (electrical double layer) and C_{Helm} (Helmholtz layer) are the most relevant for this model, including φ_{eo}, which is the potential of the electrolyte–insulator interface that determines the ISFET sensitivity face to ions concentration.

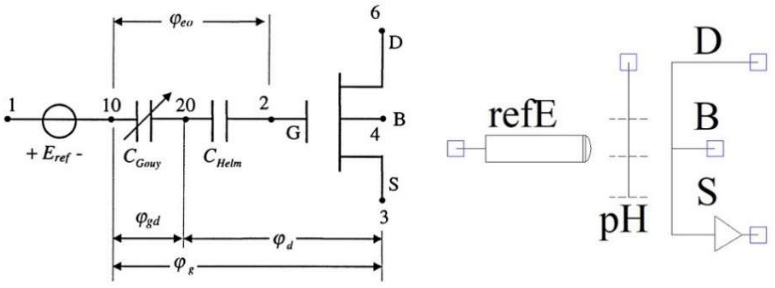

(a) (b)

Figure 8. (a) Ion-Sensitive Field Effect Transistor (ISFET) behavioral simulation macromodel (after Martinoia and Massobrio, 2000). (b) LTspice software subcircuit block used in the macromodel

Equation (7) shows that φ_{eo} is modeled as a non-linear voltage-controlled source, which depends both on pH and φ_{eo} itself. In the equation, functions $f_a(\cdot)$ and $f_b(\cdot)$ are self-explaining setting functions, N_{sil} is the surface density of the silanol sites, N_{nit} is the surface density of the amine sites, q is the charge of a proton and C_{eq} is an equivalent capacitor, which takes account of the Gouy-Chapman (Bousse et al. 1983) or electrical double layer (C_{Gouy}) and the Helmholtz layer (C_{Helm}) (Fung et al., 1986; Massobrio et al., 1994).

$$\varphi_{eo} = \frac{q}{C_{eq}}\left[N_{sil} f_a(\varphi_{eo}, pH) + N_{nit} f_b(\varphi_{eo}, pH)\right] \tag{7}$$

The electrical double layer is a structure that appears on the ISFET surface when it is exposed to a chemical solution. Meanwhile, the Helmholtz layer expresses a common boundary (interface) when two phases appear (e.g., when an electronic conductor is brought in contact with a solid or liquid ionic conductor).

Equation (8) shows the equivalent capacitor. (C_{eq}) mathematical expression composed of series capacitors C_{Gouy} and C_{Helm}: for the C_{Gouy} capacitor, q is the proton charge, ε_w is the permittivity of the electrolyte, k is the Boltzmann's constant, T is the electrolyte temperature and c_{bulk} is the ion concentration in the electrolyte; for the C_{Helm} capacitor, ε_{IHP} and ε_{OHP} are the inner and outer Helmholtz plane permittivities, respectively, d_{IHP} and d_{OHP} are the insulator–nonhydrated ion and the insulator–hydrated ion distances, respectively.

$$C_{eq} = \frac{C_{Gouy}C_{Helm}}{C_{Gouy} + C_{Helm}}, \text{with: } C_{Gouy} \cong \frac{q\sqrt{8\varepsilon_w kTc_{bulk}}}{2kT} \text{ and } C_{Helm} = \frac{\varepsilon_{IHP}\varepsilon_{OHP}}{\varepsilon_{OHP}d_{IHP} + \varepsilon_{IHP}d_{OHP}}WL \tag{8}$$

Furthermore, Figure 8(b) represents the subcircuit of the ISFET sensor, which internally has SPICE code lines (Appendix I) and associates the block inputs to generate a set of outputs from the physicochemical equations previously shown. The subcircuit was created in LTspice, a SPICE-based analog electronic circuit simulator computer software, produced by semiconductor manufacturer Analog Devices (originally by Linear Technology). The inputs are expressed in voltage through the reference electrode (E_{ref}), the pH value (pH_{input}), e.g., from 1V to 9V where 1V represents pH = 1 and 9V represents pH = 9, and the voltage between the drain terminals (Drain) and Source (Source). The macromodel output is commonly associated with the drain current I_{ds}.

6.2. Macromodel implementation

To validate the macromodel, the code proposed by Martinoia and Massobrio (2000) was implemented in the LTspice software in this paper. It was necessary to make some adjustments to the original code, written in HSPICE, to enable running the simulation in the LTspice software.

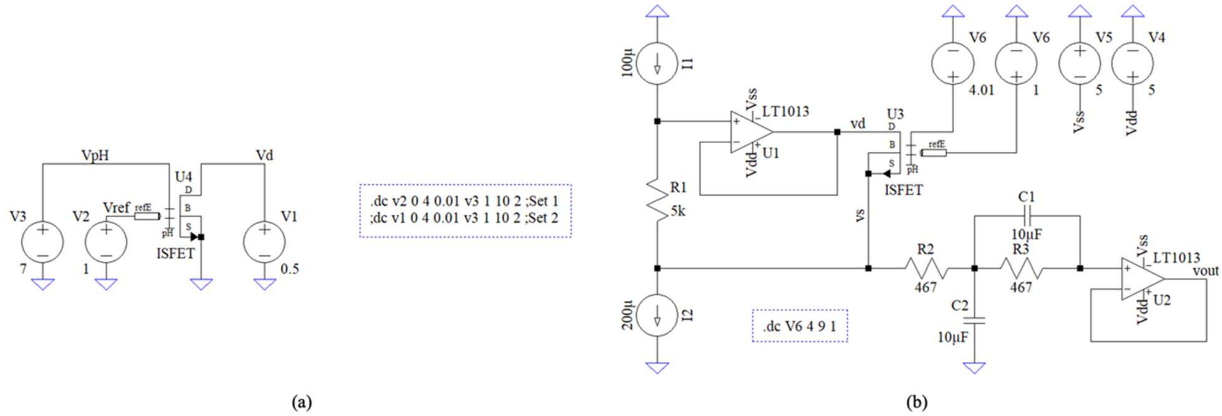

Figure 9. Ion-Sensitive Field Effect Transistor (ISFET) LTspice circuit implementation to obtain the characteristic curves. (a) circuit for ISFET I-V curves generator and (b) constant voltage constant current circuit (CVCC) readout circuit implementation

In the first instance, the simulation options must be configured because they allow an optimized convergence of the macromodel during the simulation. In the script of the Appendix, some options have not been modified, however, it is suggested to configure the following options in the control panel/ SPICE of LTspice software: Engine Solver = Alternate, Max threads = 4, Chgtol=1e-14, Trtol = 1, and Sstol = 0.0001. Once LTspice options have been adjusted, the circuit must be implemented. To validate the macromodel it is necessary to obtain the curves that show its drain-source current behavior at different voltages and pH levels. Figure 9(a) shows the circuit to get those curves. A first simulation scenario (.dc v2 0 4 0.01 v3 1 10 2) is obtained from the voltage variation of the reference electrode (V_2) and by generating different pH levels through the voltage source (V_3) and keeping constant the voltage between the drain and source with V_1 = 0.5V. As a result, a set of I_{ds}/V_{gs} curves for different pH levels are obtained (Figure 10a). The second scenario (.dc v1 0 4 0.001 v3 1 10 2) is based on the variation of the drain-source voltage (V_1), keeping the reference electrode voltage constant with V_2 = 1V and again, generating different pH levels through the voltage source (V_3). Here, I_{ds}/V_{ds} curves are obtained for different pH levels (Figure 10b). These curves from both scenarios are significant because they allow distinguishing between the linear region and the saturated region of the ISFET sensor regions, which allow selecting the operation points to implement readout circuits.

A CVCC circuit is shown in Figure 9(b) and the results of its simulation are shown in Figure 10(c). In the circuit, a voltage $V_{ds} = 0.5V$ is generated with the current source I_1 and the resistor R1, that is, 100 µA·5kΩ = 0.5V. This voltage goes through a voltage follower made with the opamp LT1013 from Analog Devices. The current I_{ds} is kept constant through the current source I_2 and this is verified by the Kirchhoff's current law $I_1 + I_{ds} = I_2$, which is 100µA + 100µA = 200µA at the source node. Once the values of Ids and Vds are kept constant, an output signal (V_{out}) proportional to the changes in pH is obtained. This output signal, which corresponds to a voltage, is filtered through an active low-pass filter in Sallen-Key topology using resistors, capacitors, and the OPAMP LT1013.

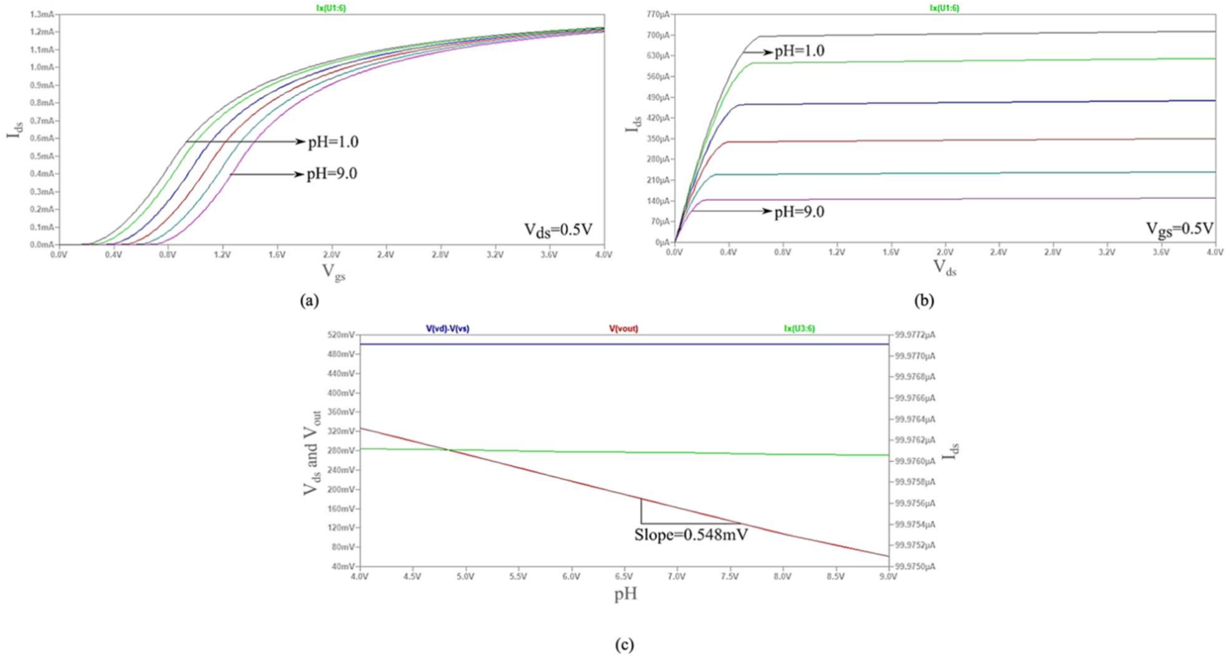

Figure 10. (a) Characteristics curves for V_{gs} vs I_{ds} with $V_{ds} = 0.5V$, (b) Characteristics curves for V_{ds} vs I_{ds} with $V_{gs} = 0.1V$, and (c) Constant voltage constant current circuit (CVCC) readout

Finally, the behavior of the CVCC circuit is obtained through the simulation command (.dc V6 4 9 1), which generates a variation from pH = 4 to pH = 9 through the V_6 source. Figure. 10(c) shows the constant values of V_{ds} = 500.060 mV and I_{ds} = 99.9762uA. The output voltage V_{out}, which goes from 60mV to

330mV, follows a Nernstian slope with an approximate value of -0.0548mV/pH, which corroborates the correct implementation of the model.

It can be concluded that the macromodel simulation is necessary for two reasons: 1) to obtain the I_{ds}/V_{ds} and I_{ds}/V_{gs} curves of the ISFET sensor and 2) to verify the sensor performance with the electronic instrumentation stages or readout circuits. In the first instance, the I_{ds}/V_{ds} and I_{ds}/V_{gs} simulation is relevant for cases where there is no curve tracer equipment and if the idea is to know the operating points of the sensor. This task requires prior knowledge of the approximate values of the physical parameters of the ISFET sensor (e.g., W, L, C_{ox}, etc.). Every readout circuit design requires a simulation phase. Whether to implement a new readout circuit or an existing one, implementing the ISFET macromodel in a readout circuit simulation allows knowing approximately if the sensor is coupled to the circuit conditions, avoiding possible failures or damage at the time of implementation on a PCB.

7. Conclusions

Issues related to ISFET basic principles, electronic instrumentation, and non-idealities including their application potential for the analyses of soil nutrients in PA context were reviewed. Few research and development gaps were highlighted. Although the literature offers a wide range of applications of ISFET sensors in other domains, there are only few use examples for the measurement of the available fraction of macronutrients and pH in agricultural soils. The on-the-go and stationary sensing platforms using ISFET or ISE technologies can be adopted to generate useful information on available nutrients necessary for precision management of soil fertility through site specific fertilization and manure application. They are fast, direct methods of soil solution analysis, and cheap, compared to the classical methods of laboratory analyses that are difficult, expensive, slow and expose chemical agents into the environment. Due its mobility and portability nature, ISFET allows the generation of large volumes of information to better understand the spatiotemporal variability, for variable rate application. The review revealed that more research is needed to allow ISFET sensing technology to find its way for practical application in PA. Future development is necessary to overcome few shortcomings related to the lag time, stability of the sensor readings, non-idealities, and robustness.

Knowledge gained in the biomedical field can be transferred to PA applications. As ISFET are subjected to a set of non-idealities such as trapped charge, drift, noise, and intrinsic temperature, adaptation of the sensor design, integrating compensation systems and using electronic instrumentation are necessary mitigation solutions. However, the characterization of these non-idealities and their compensation must be approached in the context of agricultural soils, for which more studies are required.

The modeling and simulation are important aspects that allow in depth understanding of the ISFET behavior. Simulations by macromodels allow the validation of electronic systems design in a cost-effective and fast manner. However, more research is needed to generate new macromodels that simulate the ISFET behavior for the detection of agricultural soil nutrients e.g., nitrate, potassium, and phosphate, including non-idealities. Such improved modelling approach will allow development of ISFET sensors suitable for on-the-go and stationary data collections on soil nutrients and pH for PA applications.

Appendix

The adaptation of the code of SPICE macromodel of Martinoia and Massobrio (2000) for the simulation of ISFET sensor behavior using LTSPICE software:

```
************************************************
ISFET macromodel adaptation for LTSPICE simulations
Original version from Martinoia and Massobrio, (2000)
************************************************

**********Simulator parameters**********************
+ abstol = 1e-15
+ pivrel = 1e-13
+ pivtol = 1e-13
+ vntol = 0.000001
+ reltol = 1e-12
+ Gmin = 1e-24 itl1 = 1000
+ srcstepmethod = 2
+ method = gear itl4 = 10000 MinDeltaGmin = 1e-15
+ maxstep = 0.2
**********Model parameters**************************
.PARAM
```

```
+ k = 1.38e-23 T = 300 eps0 = 8.85e-12
+ Ka = 15.8 Kb = 63.1e-9 Kn = 1e-10
+ Nsil = 3e18 Nnit = 2e18
+ Cbulk = 0.1
+ q = 1.6e-19 NAv = '6.023e23*1e3'
+ epsw = 78.5 epsihp = 32 epsohp = 32
+ dihp = 0.1n dohp = 0.3n
+ Eabs = 4.7 Phim = 4.7 Erel = 0.200 Chieo = 3e-3 Philj = 1e-3
+ ET = 'q/(k*T)'
+ sq = 'sqrt(8*eps0*epsw*k*T)'
+ Cb = 'NAv*Cbulk'
+ KK = 'Ka*Kb'
+ Ch = '((eps0*epsihp*epsohp)/(epsohp*dihp+epsihp*dohp))'
+ Cd = '(sq*ET*0.5)*sqrt(Cb)'
+ Ceq = '1/((1/Cd)+(1/Ch))'

********** Beginning of the sub-circuit definition*********
.SUBCKT ISFET 6 1 3 4 101
*drain=6 | ref.el=1 | source =3| bulk =4| pH input=101
Eref 1 10 VALUE = {Eabs-Phim-Erel+Chieo+Philj}
Ceq 10 2 {1/((1/Cd)+(1/Ch))}
EP1 46 0 VALUE = {log(KK)+(4.6*V(101))}
RP1 46 0 1G
EP2 23 0 VALUE = {log(Ka)+(2.3*V(101))}
RP2 23 0 1G
EPH 2 10 VALUE = {(q/Ceq)*(Nsil*((exp(-2*V(2,10)*ET)-exp(V(46)))/(exp(-2*V(2,10)*ET)+exp(V(23))*exp(-
1*V(2,10)*ET)+exp(V(46))))+Nnit*((exp(-1*V(2,10)*ET))/exp(-1*V(2,10)*ET)+(Kn/Ka)*exp(V(23))))}
RpH 101 0 1K
*MIS 6 2 3 4 MISFET L = 10u W = 900u NRS = 5 NRD = 5
MIS 6 2 3 4 MISFET L = 10u W = 840u NRS = 5 NRD = 5

********** MOSFET model ***************************
.MODEL MISFET NMOS LEVEL = 2
+           VTO = 7.99e-1 LAMBDA = 7.59e-3 RSH = 3.5e1 TOX = 86e-9
+           UO = 6.53e+2 TPG = 0
+           UEXP = 7.64e-2 NSUB = 3.27e+15 NFS = 1.21e11
+           NEFF = 3.88 VMAX = 5.35e4 DELTA = 1.47 LD = 2.91e-6
+           UCRIT = 7.97e4 XJ = 6.01e-9 CJ = 4.44e-4 IS = 1e-11
+           CJSW = 5.15e-10 PHI = 5.55e-1 GAMMA = 9.95e-1
+           MJ = 0.395 MJSW = 0.242 PB = 0.585
****************************************************
.ENDS ISFET
```

Acknowledgments

This work was supported by Gobernación de Bolívar, Colombia, and the program "Bolívar Gana con Ciencia". Authors acknowledge the financial support received from the Research Foundation - Flanders (FWO) for Odysseus I SiTeMan Project (Nr. G0F9216N).

References

Abu Samah, Nur Liyana Mardhiah, Khuan Y. Lee, and Roziah Jarmin. 2016. "H+ Ion-Sensitive FET Macromodel in LTSPICE IV." Journal of Computational Electronics 15(4):1407–15. https://doi.org/10.1007/s10825-016-0919-x.

Adamchuk, V. I., J. W. Hummel, M. T. Morgan, and S. K. Upadhyaya. 2004. “On-the-Go Soil Sensors for Precision Agriculture.” Computers and Electronics in Agriculture 44(1):71–91. https://doi.org/10.1016/j.compag.2004.03.002.

Adamchuk, V. I., M. T. Morgan, and D. R. Ess. 1999. “An Automated Sampling System for Measuring Soil PH.” Transactions of the ASAE, 42(4), 885-892. https://doi.org/10.13031/2013.13268.

Adamchuk, Viacheslav I., Eric D. Lund, Todd M. Reed, and Richard B. Ferguson. 2007. “Evaluation of an On-the-Go Technology for Soil PH Mapping.” Precision Agriculture 8(3):139–49. https://doi.org/10.1007/s11119-007-9034-0 .

Adsett, J. F., J. A. Thottan, and K. J. Sibley. 1999. “Development of an Automated On-The-Go Soil Nitrate Monitoring System.” Applied Engineering in Agriculture 15(902):351–56. https://doi.org/10.13031/2013.5789.

Afriyie Ernest, Ann Verdoodt, and Abdul M. Mouazen. 2021. “Data Fusion of Visible Near-Infrared and Mid-Infrared Spectroscopy for Rapid Estimation of Soil Aggregate Stability Indices.” Computers and Electronics in Agriculture 187(September 2020):106229. https://doi.org/10.1016/j.compag.2021.106229.

Ali, Md. A., Dong Liang, Dhau Jaspreet., Khosla Ajit, & Kaushik Ajeet. (2020). Perspective—Electrochemical sensors for soil quality assessment. Journal of The Electrochemical Society, 167(3), 037550. https://doi.org/10.1149/1945-7111/ab69fe.

Ali Md. Azahar, Xinran Wang, Yuncong Chen, Yueyi Jiao, Navreet K. Mahal, Satyanarayana Moru, Michael J. Castellano, James C. Schnable, Patrick S. Schnable, and Liang Dong. 2019. “Continuous Monitoring of Soil Nitrate Using a Miniature Sensor with Poly(3-Octyl-Thiophene) and Molybdenum Disulfide Nanocomposite.” ACS Applied Materials and Interfaces 11(32):29195–206. https://doi.org/10.1021/acsami.9b07120.

Archbold Taylor, G., Beltran Torres, H., Ruiz, F., Narducci Marin, M., Mendez Chaves, D., Trujillo Arboleda, L., Parra, C., Carrillo, H., & Mouazen, A. M. (2019). pH measurement IoT system for precision agriculture applications. IEEE Latin America Transactions, 17(05), 823-832. https://doi.org/10.1109/TLA.2019.8891951.

Archbold Taylor, G. A., Parra, C., Carrillo, H., & Mouazen, A. (2020). A decision framework reference for ISFET sensor-based electronic systems design for agriculture industry applications. 2020 IEEE 17th India Council International Conference (INDICON), 1-6. https://doi.org/10.1109/INDICON49873.2020.9342231.

Artigas, J., Beltran, A., Jiménez, C., Baldi, A., Mas, R., Domínguez, C., & Alonso, J. (2001). Application of ion sensitive field effect transistor based sensors to soil analysis. Computers and Electronics in Agriculture, 31(3), 281-293. https://doi.org/10.1016/S0168-1699(00)00187-3.

Baldi, A., A. Bratov, R. Mas, and C. Domínguez. 2001. “Electrostatic Discharge Sensitivity Tests for ISFET Sensors.” Sensors and Actuators, B: Chemical 80(3):255–60. https://doi.org/10.1016/S0925-4005(01)00918-2.

Belkhamssa, N., Justino, C. I. L., Santos, P. S. M., Cardoso, S., Lopes, I., Duarte, A. C., Rocha-Santos, T., & Ksibi, M. (2016). Label-free disposable immunosensor for detection of atrazine. Talanta, 146, 430-434. https://doi.org/10.1016/j.talanta.2015.09.015.

Bergveld, P. 1970. “Development of an Ion-Sensitive Solid-State Device for Neurophysiological Measurements.” IEEE Transactions on Biomedical Engineering (January):70–71. https://doi.org/10.1109/TBME.1970.4502688.

Bergveld, P. 1981. “The Operation of an Isfet as an Electronic Device.” Sensors and Actuators, B: Chemical 1:17–29. https://doi.org/10.1016/0250-6874(81)80004-2

Bergveld, P. 2003. “Thirty Years of ISFETOLOGY What Happened in the Past 30 Years and What May Happen in the next 30 Years.” Sensors & Actuators: B. Chemical 88:1–20. https://doi.org/10.1016/S0925-4005(02)00301-5.

Bergveld, Piet. 1972. “Development, Operation, and Application of the Ion-Sensitive Field-Effect Transistor as a Tool for Electrophysiology.” IEEE Transactions on Biomedical Engineering 19(5):342–51. doi: https://doi.org/10.1109/TBME.1972.324137.

Berto, M., Vecchi, E., Baiamonte, L., Condò, C., Sensi, M., Di Lauro, M., Sola, M., De Stradis, A., Biscarini, F., Minafra, A., & Bortolotti, C. A. (2019). Label free detection of plant viruses with organic transistor biosensors. Sensors and Actuators B: Chemical, 281, 150-156. https://doi.org/10.1016/j.snb.2018.10.080

Bhat, K. S., Nakate, U. T., Yoo, J.-Y., Wang, Y., Mahmoudi, T., & Hahn, Y.-B. (2019). Nozzle-jet-printed silver/graphene composite-based field-effect transistor sensor for phosphate ion detection. ACS Omega, 4(5), 8373-8380. https://doi.org/10.1021/acsomega.9b00559

Birrell, S. J., and J. W. Hummel. 2001. “Real-Time Multi ISFET / FIA Soil Analysis System with Automatic Sample Extraction.” Analytica Chimica Acta 32:45–67. https://doi.org/10.1016/S0168-1699(01)00159-4.

Bousse, Luc, Luc Bousse, Nico F. De Rood, and Piet Bergveld. 1983. “Operation of Chemically Sensitive Field-Effect Sensors As a Function of the Insulator-Electrolyte Interface.” IEEE Transactions on Electron Devices 30(10):1263–70. https://doi.org/10.1109/T-ED.1983.21284.

Burton, Lamar, K. Jayachandran, and S. Bhansali. 2020. “Review—The ‘Real-Time’ Revolution for In Situ Soil Nutrient Sensing.” Journal of The Electrochemical Society 167(3):037569. https://doi.org/10.1149/1945-7111/ab6f5d.

Carrillo-Martínez, Luis A., G. Espinosa Flores-Verdad, B. M. Pérez, and J. Molina Reyes. 2016. “pH ISFET Sensor with PVTA Compensation.” Electronic Letters 52(1). https://doi.org/10.1049/el.2015.2573.

Chan, P. K., and D. Y. Chen. 2007. “A CMOS ISFET Interface Circuit with Dynamic Current Temperature Compensation Technique.” IEEE Transactions on Circuits and Systems I: Regular Papers 54(1):119–29. https://doi.org/10.1109/TCSI.2006.887977 .

Chen, D. Y., and P. K. Chan. 2008. “An Intelligent ISFET Sensory System with Temperature and Drift Compensation for Long-Term Monitoring.” IEEE Sensors Journal 8(12):1948–59. https://doi.org/10.1109/JSEN.2008.2006471.

Chen, Ming, Miao Zhang, Xuming Wang, Qingliang Yang, Maohua Wang, Gang Liu, and Lan Yao. 2020. “An All-Solid-State Nitrate Ion-Selective Electrode Nutrient Monitoring.” Sensors. https://doi.org/10.3390/s20082270.

Chin, Yuan Lung, Jung Chuan Chou, Tai Ping Sun, Wen Yaw Chung, and Shen Kan Hsiung. 2001. “A Novel PH Sensitive ISFET with on Chip Temperature Sensing Using CMOS Standard Process.” Sensors and Actuators, B: Chemical 76(1–3):582–93. https://doi.org/10.1016/S0925-4005(01)00639-6.

Chou, Jung Chuan, Yii Fang Wang, and Jin Sung Lin. 2000. “Temperature Effect of A-Si:H pH-ISFET.” Sensors and Actuators, B: Chemical 62(2):92–96. https://doi.org/10.1016/S0925-4005(99)00369-X .

Chung, W., C. Yang, D. G. Pijanowska, A. Krzyskow, and W. Torbicz. 2004. “ISFET Interface Circuit Embedded with Noise Rejection Capability.” Electronics Letters, vol. 40, 18. https://doi.org/10.1049/el:20045388.

Chung, Wen-yaw, Yeong-tsair Lin, Dorota G. Pijanowska, Chung-huang Yang, Ming-chia Wang, Alfred Krzyskow, and Wladyslaw Torbicz. 2006. “New ISFET Interface Circuit Design with Temperature Compensation.” Microelectronics Journal 37:1105–14. https://doi.org/10.1016/j.mejo.2006.05.001.

Cumming, D. R. S. 2011. “ISFET Technology for Multi-Sensor Technology : From Lab-in-a-Pill to Massively Parallel Measurements.” 14–16. https://doi.org/10.1049/el.2011.2891.

Dam, Van Anh T., and Marcel A. G. Zevenbergen. 2019. “Low cost nitrate sensor for agricultural applications.” 2019 20th International Conference on Solid-State Sensors, Actuators and Microsystems & Eurosensors XXXIII (Transducers & Eurosensors XXXIII) (June):1285–88. https://doi.org/10.1109/TRANSDUCERS.2019.8808327.

Das, M. P., M. Bhuyan, and C. Talukdar. 2015. “Readout Circuits for Noise Compensation in ISFET Sensory System.” Sensing and Imaging 16(1). https://doi.org/10.1007/s11220-014-0103-y.

De Santana, Felipe B., Larissa O. de Giuseppe, André M. de Souza, and Ronei J. Poppi. 2019. “Removing the Moisture Effect in Soil Organic Matter Determination Using NIR Spectroscopy and PLSR with External Parameter Orthogonalization.” Microchemical Journal, 145: 1094–1101. https://doi.org/10.1016/j.microc.2018.12.027 .

Dei, Michele, Joan Aymerich, Massimo Piotto, Paolo Bruschi, Francisco del Campo, and Francesc Serra-Graells. 2019. “CMOS Interfaces for Internet-of-Wearables Electrochemical Sensors: Trends and Challenges.” Electronics 8(2):150. https://doi.org/10.3390/electronics8020150.

Diacci, C., Abedi, T., Lee, J. W., Gabrielsson, E. O., Berggren, M., Simon, D. T., Niittylä, T., & Stavrinidou, E. (2021). Diurnal in vivo xylem sap glucose and sucrose monitoring using implantable organic electrochemical transistor sensors. IScience, 24(1), 101966. https://doi.org/10.1016/j.isci.2020.101966.

Dzyadevych, Sergei V., Alexey P. Soldatkin, Anna V. El’skaya, Claude Martelet, and Nicole Jaffrezic-Renault. 2006. “Enzyme Biosensors Based on Ion-Selective Field-Effect Transistors.” Analytica Chimica Acta 568(1–2):248–58. https://doi.org/10.1016/j.aca.2005.11.057.

Eggins, Brian R. 2002. Chemical Sensors and Biosensors. John Wiley and Sons.

Elli, G., Hamed, S., Petrelli, M., Ibba, P., Ciocca, M., Lugli, P., & Petti, L. (2022). Field-effect transistor-based biosensors for environmental and agricultural monitoring. Sensors, 22(11), 4178. https://doi.org/10.3390/s22114178.

Erler, Alexander, Daniel Riebe, Toralf Beitz, Hans Gerd Löhmannsröben, and Robin Gebbers. 2020. “Soil Nutrient Detection for Precision Agriculture Using Handheld Laser-Induced Breakdown Spectroscopy (LIBS) and

Multivariate Regression Methods (PLSR, Lasso and GPR).” Sensors (Switzerland) 20(2). https://doi.org/10.3390/s20020418.

Fernandes, Poornika G., Harvey J. Stiegler, Mingyue Zhao, Kurtis D. Cantley, Borna Obradovic, Richard A. Chapman, Huang Chun Wen, Gazi Mahmud, and Eric M. Vogel. 2012. “SPICE Macromodel of Silicon-on-Insulator-Field-Effect-Transistor-Based Biological Sensors.” Sensors and Actuators, B: Chemical 161(1):163–70. https://doi.org/10.1016/j.snb.2011.10.002.

Fung, C. D., P. W. Cheung, and W. H. Ko. 1986. “A Generalized Theory of an Electrolyte-Insulator-Semiconductor Field-Effect Transistor.” IEEE Transactions on Electron Devices 33(1):8–18. https://doi.org/10.1109/T-ED.1986.22429.

Gao, R., & Lloyd, J. (2020). Precision and accuracy: Knowledge transformation through conceptual learning and inquiry-based practices in introductory and advanced chemistry laboratories. Journal of Chemical Education, 97(2), 368-373. https://doi.org/10.1021/acs.jchemed.9b00563.

Gràcia, I., C. Cane, M. Lozano, and J. Esteve. 1992. “Test Structures for ISFET Chemical Sensors.” ICMTS 92 Proceedings of the 1992 International Conference on Microelectronic Test Structures 5(March):156–59. https://doi.org/10.1109/ICMTS.1992.185959.

Guerrero, Angela, Stefaan De Neve, and Abdul M. Mouazen. 2021. Current Sensor Technologies for in Situ and On-Line Measurement of Soil Nitrogen for Variable Rate Fertilization: A review. Advances in Agronomy, 168, 1-38. https://doi.org/10.1016/bs.agron.2021.02.001.

Guerrero, E., Carrillo-Martínez, L. A., Sanz-Pascual, M. T., Molina, J., Medrano, N., & Calvo, B. (2013). Offset and gain calibration circuit for MIM-ISFET devices. Analog Integrated Circuits and Signal Processing, 76(3), 321-333. https://doi.org/10.1007/s10470-013-0077-z.

Hamimed, S., Mahjoubi, Y., Abdeljelil, N., Gamraoui, A., Othmani, A., Barhoum, A., & Chatti, A. (2023). Chemical sensors and biosensors for soil analysis: Principles, challenges, and emerging applications. En Advanced Sensor Technology (pp. 669-698). Elsevier. https://doi.org/10.1016/B978-0-323-90222-9.00014-5.

He, Minghuai, Nicolas Moser, and Pantelis Georgiou. 2020. “A Multi-Sensing Pixel for Integrated Opto-Chemical Sensing with Temperature Compensation.” (1):1–5. https://doi.org/10.1109/iscas45731.2020.9181098.

Hinck, S., Möller, A., Mentrup, D., Najdenko, E., Lorenz, F., Mosler, T., & Ruckelshausen, A. (2018). soil2data: Concept for a mobile field laboratory for nutrient analysis. Proceedings of the 14th ICPA. Montreal, Canada.

Hong, Y., Chung, S.-O., Park, J., & Hong, Y. (2022). Portable soil ph sensor using isfet electrode. Journal of Information and Communication Convergence Engineering, 20(1), 49-57. https://doi.org/10.6109/JICCE.2022.20.1.49.

Huang, Xiwei, Hao Yu, Senior Member, Xu Liu, and Yu Jiang. 2015. “A Dual-Mode Large-Arrayed CMOS ISFET Sensor for Accurate and High-Throughput PH Sensing in Biomedical Diagnosis.” IEEE Transactions on Biomedical Engineering 62(9):2224–33. https://doi.org/10.1109/TBME.2015.2419233.

Ishige, Yu, Maki Shimoda, and Masao Kamahori. 2009. “Extended-Gate FET-Based Enzyme Sensor with Ferrocenyl-Alkanethiol Modified Gold Sensing Electrode.” Biosensors and Bioelectronics 24(5):1096–1102. https://doi.org/10.1016/j.bios.2008.06.012.

Ito, Yoshitaka. 2000. “Stability of ISFET and Its New Measurement Protocol.” Sensors and Actuators, B: Chemical 66(1):53–55. https://doi.org/10.1016/S0925-4005(99)00443-8.

Jamasb, Shahriar. 2004. “An Analytical Technique for Counteracting Drift in Ion-Selective Field Effect Transistors (ISFETs).” IEEE Sensors Journal 4(6):795–801. https://doi.org/10.1109/JSEN.2004.833148.

Javadi, S. H., Munnaf, M. A., & Mouazen, A. M. (2021). Fusion of Vis-NIR and XRF spectra for estimation of key soil attributes. Geoderma, https://doi.org/10.1016/j.geoderma.2020.114851.

Ji, W., Adamchuk, V. I., Chen, S., Mat Su, A. S., Ismail, A., Gan, Q., Shi, Z., & Biswas, A. (2019). Simultaneous measurement of multiple soil properties through proximal sensor data fusion: A case study. Geoderma, 341, 111-128. https://doi.org/10.1016/j.geoderma.2019.01.006.

Joly, M., Marlet, M., Durieu, C., Bene, C., Launay, J., & Temple-Boyer, P. (2022). Study of chemical field effect transistors for the detection of ammonium and nitrate ions in liquid and soil phases. Sensors and Actuators B: Chemical, 351, 130949. https://doi.org/10.1016/j.snb.2021.130949.

Kaisti, Matti. 2017. “Detection Principles of Biological and Chemical FET Sensors.” Biosensors and Bioelectronics 98(June):437–48. https://doi.org/10.1016/j.bios.2017.07.010.

Kashyap, B., & Kumar, R. (2021). Sensing methodologies in agriculture for soil moisture and nutrient monitoring. IEEE Access, 9, 14095-14121. https://doi.org/10.1109/ACCESS.2021.3052478.

Kalofonou, Melpomeni, and Christofer Toumazou. 2014. “A Low Power Sub-MW Chemical Gilbert Cell for Isfet Differential Reaction Monitoring.” IEEE Transactions on Biomedical Circuits and Systems 8(4):565–74. https://doi.org/10.1109/TBCAS.2013.2282894.

Khanna, V. K., Wolfram Oelßner, and Ulrich Guth. 2009. “Interfacial and Adhesional Aspects in Polyurethane (PUR) Membrane Coating on Si3N4 Surface of ISFET Gate for REFET Fabrication.” Applied Surface Science 255(17):7798–7804. https://doi.org/10.1016/j.apsusc.2009.04.182.

Kim, Hak-Jin, John W. Hummel, Kenneth A. Sudduth, and Peter P. Motavalli. 2007. “Simultaneous Analysis of Soil Macronutrients Using Ion-Selective Electrodes.” Soil Science Society of America Journal 71(6):1867. https://doi.org/10.2136/sssaj2007.0002.

Kuang, Boyan, Hafiz S. Mahmood, Mohammed Z. Quraishi, Willem B. Hoogmoed, and Abdul M. Mouazen. 2012. Sensing Soil Properties in the Laboratory , In Situ , and On-Line : A Review. Sensing soil properties in the laboratory, in situ, and on-line: a review. Advances in agronomy, 114, 155-223. https://doi.org/10.1016/B978-0-12-394275-3.00003-1.

Le Bris, N., and D. Birot. 1997. “Automated PH-ISFET Measurements under Hydrostatic Pressure for Marine Monitoring Application.” Analytica Chimica Acta 356(2–3):205–15. doi: 10.1016/S0003-2670(97)00533-3.

Lehmann, Ulrike, and Alain Grisel. 2014. “Miniature Multisensor Probe for Soil Nutrient Monitoring.” Procedia Engineering 87:1429–32. https://doi.org/10.1016/j.proeng.2014.11.713.

Lin, J., Wang, M., Zhang, M., Zhang, Y., Chen, L. (2008). Electrochemical Sensors for Soil Nutrient Detection: Opportunity and Challenge. In: Li, D. (eds) Computer And Computing Technologies In Agriculture, Volume II. CCTA 2007. The International Federation for Information Processing, vol 259. Springer, Boston, MA. https://doi.org/10.1007/978-0-387-77253-0_77.

Liu, J., Dong, Z., Xia, J., Wang, H., Meng, T., Zhang, R., Han, J., Wang, N., & Xie, J. (2021). Estimation of soil organic matter content based on CARS algorithm coupled with random forest. Spectrochimica Acta Part A: Molecular and Biomolecular Spectroscopy, 258, 119823. https://doi.org/10.1016/j.saa.2021.119823.

Lobsey, Craig, Raphael Viscarra Rossel, and Alex McBratney. 2010. "An Automated System for Rapid In-Field Soil Nutrient Testing Craig." in 19th World Congress of Soil Science, Soil Solutions for a Changing World. Brisbane, Australia.

Lund, E. D., Collings, K. L., Drummond, P. E., Christy, C. D., & Adamchuk, V. I. (2004). Managing pH variability with on-the-go pH mapping. In Proceedings of the seventh international conference on precision agriculture. ASA, CSSA, and SSSA, Madison, WI.

Martinoia, Sergio, and Giuseppe Massobrio. 2000. "Behavioral Macromodel of the ISFET in SPICE." Sensors and Actuators, B: Chemical 62(3):182–89. https://doi.org/10.1016/S0925-4005(99)00377-9.

Martinoia, Sergio, Giuseppe Massobrio, and Leandro Lorenzelli. 2005. "Modeling ISFET Microsensor and ISFET-Based Microsystems: A Review." Sensors and Actuators, B: Chemical 105(1):14–27. https://doi.org/10.1016/j.snb.2004.02.046.

Martz, Todd R., James G. Connery, and Kenneth S. Johnson. 2010. "Testing the Honeywell Durafet® for Seawater PH Applications." Limnology and Oceanography: Methods 8(MAY):172–84. https://doi.org/10.4319/lom.2010.8.172.

Massobrio, Giuseppe, Sergio Martinoia, and Massimo Grattarola. 1994. "Use of SPICE for Modeling Silicon-Based Chemical Sensors." Sensors and Materials, Vol. 6, No. 2, 1994, p. 101-124.

Milgrew, M. J., P. A. Hammond, and D. R. S. Cumming. 2004. "The Development of Scalable Sensor Arrays Using Standard CMOS Technology." Sensors and Actuators, B: Chemical 103:37–42. doi: 10.1016/j.snb.2004.03.004.

Milgrew, Mark J., and D. R. S. Cumming. 2008. "Matching the Transconductance Characteristics of CMOS ISFET Arrays by Removing Trapped Charge." IEEE Transactions on Electron Devices 55(4):1074–79. https://doi.org/10.1109/TED.2008.916680.

Morellos, Antonios, Xanthoula Eirini Pantazi, Dimitrios Moshou, Thomas Alexandridis, Rebecca Whetton, Georgios Tziotzios, Jens Wiebensohn, Ralf Bill, and Abdul M. Mouazen. 2016. "Machine Learning Based Prediction of Soil Total Nitrogen, Organic Carbon and Moisture Content by Using VIS-NIR Spectroscopy." Biosystems Engineering 152:104–16. https://doi.org/10.1016/j.biosystemseng.2016.04.018.

Morgenshtein, Arkagiy. 2003. Design and methodology of ISFET (Ion sensitive field effect transistor) microsystems for bio-telemetry: Technion-Israel Institute of Technology, Department of Biomedical Engineering, 2003.

Morgenshtein, Arkadiy, Liby Sudakov-boreysha, Uri Dinnar, Claudio G. Jakobson, and Yael Nemirovsky. 2004a. "CMOS Readout Circuitry for ISFET Microsystems." 97:122–31. https://doi.org/10.1016/j.snb.2003.08.007.

Morgenshtein, Arkadiy, Liby Sudakov-boreysha, Uri Dinnar, Claudio G. Jakobson, and Yael Nemirovsky. 2004b. "Wheatstone-Bridge Readout Interface for ISFET / REFET Applications." 98:18–27. https://doi.org/10.1016/j.snb.2003.07.017.

Moser, Nicolas, Tor Sverre Lande, Christofer Toumazou, and Pantelis Georgiou. 2016. “ISFETs in CMOS and Emergent Trends in Instrumentation: A Review.” IEEE Sensors Journal 16(17):6496–6514. https://doi.org/10.1109/JSEN.2016.2585920.

Mouazen, A.M. Soil Survey Device 2006. In International Publication, Published under the Patent Cooperation Treaty (PCT); World Intellectual Property Organization, International Bureau: Brussels, Belgium, 2006.

Mouazen, A., Alexandridis, T., Buddenbaum, H., Cohen, Y., Moshou, D., Mulla, D., … Sudduth, K. A. (2020). Monitoring. In A. Castrignanò, G. Buttafuoco, R. Khosla, A. Mouazen, D. Moshou, & O. Naud (Eds.), Agricultural Internet of Things and decision support for precision smart farming (pp. 35–138). https://doi.org/10.1016/b978-0-12-818373-1.00002-0.

Mugo, S. M., Lu, W., & Lemieux, S. (2022). Stainless steel electrochemical capacitive microneedle sensors for multiplexed simultaneous measurement of pH, nitrates, and phosphates. Microchimica Acta, 189(5), 206. https://doi.org/10.1007/s00604-022-05307-4.

Nadporozhskaya, M., Kovsh, N., Paolesse, R., & Lvova, L. (2022). Recent advances in chemical sensors for soil analysis: A review. Chemosensors, 10(1), 35. https://doi.org/10.3390/chemosensors10010035.

Nawar, Said, Muhammad Abdul Munnaf, and Abdul Mounem Mouazen. 2020. “Machine Learning Based On-Line Prediction of Soil Organic Carbon after Removal of Soil Moisture Effect.” Remote Sensing 12(8). https://doi.org/10.3390/RS12081308.

Palán, B., F. V. Santos, J. M. Karam, B. Courtois, and M. Husák. 1999. “New ISFET Sensor Interface Circuit for Biomedical Applications.” Sensors and Actuators, B: Chemical 57(1–3):63–68. https://doi.org/10.1016/S0925-4005(99)00136-7.

Patil, Sheetal, Hemant Ghadi, Niranjan Ramgir, Arindam Adhikari, and V. Ramgopal Rao. 2019. “Monitoring Soil PH Variation Using Polyaniline/SU-8 Composite Film Based Conductometric Microsensor.” Sensors and Actuators, B: Chemical 286(October 2018):583–90. https://doi.org/10.1016/j.snb.2019.02.016.

Patkar, R. S., Ashwin, M., & Rao, V. R. (2017). Piezoresistive microcantilever based lab-on-a-chip system for detection of macronutrients in the soil. Solid-State Electronics, 138, 94-100. https://doi.org/10.1016/j.sse.2017.07.007.

Premanode, B., Silawan, N., & Toumazou, C. (2007). Drift reduction in ion-sensitive FETs using correlated double sampling. Electronics Letters, 43(16), 1. https://doi.org/10.1049/el:20071118.

Rosenberg, Ron, Michael S. Bono, Soumya Braganza, Chintan Vaishnav, Rohit Karnik, and A. John Hart. 2018. “In-Field Determination of Soil Ion Content Using a Handheld Device and Screen-Printed Solidstate Ion-Selective Electrodes.” PLoS ONE 13(9):1–20. https://doi.org/10.1371/journal.pone.0203862.

Behera, S. K., Adamchuk, V. I., Shukla, A. K., Pandey, P. S., Kumar, P., Shukla, V., Thiyagarajan, C., Rai, H. K., Hadole, S., Sachan, A. K., Singh, P., Trivedi, V., Mishra, A., Butail, N. P., Kumar, P., Prajapati, R., Tiwari, K., Suri, D., & Sharma, M. (2022). The scope for using proximal soil sensing by the farmers of india. Sustainability, 14(14), 8561. https://doi.org/10.3390/su14148561.

Roziah Jarmin, R., Lee Yoot Khuan, Hadzli Hashim, Anuar Ahmad, and Mohd Mazzuan. 2010. “A New PSpice Macro Model for Electrolyte Insulator Interface Based Si3N4 Field Effect Transistor Responsive to H+ Ion

Concentration for Biomedical Sensor.” Proceedings of 2010 IEEE EMBS Conference on Biomedical Engineering and Sciences, IECBES 2010 (December):505–8. https://doi.org/10.1109/IECBES.2010.5742290.

Ruane, John, and Andrea Sonnino. 2010. “Agricultural Biotechnologies in Developing Countries and Their Possible Contribution to Food Security.” Journal of Biotechnology 156(4):356–63. https://doi.org/10.1016/j.jbiotec.2011.06.013.

Schirrmann, Michael, Robin Gebbers, Eckart Kramer, and Jan Seidel. 2011. “Soil PH Mapping with an On-the-Go Sensor.” Sensors 11(1):573–98. https://doi.org/10.3390/s110100573.

Sentek. 2018. “Ion-Selective-Electrode Manual Nitrate SENTEK.”

Sethuramasamyraja, B., V. I. Adamchuk, A. Dobermann, D. B. Marx, D. D. Jones, and G. E. Meyer. 2008. “Agitated Soil Measurement Method for Integrated On-the-Go Mapping of Soil PH, Potassium and Nitrate Contents.” Computers and Electronics in Agriculture 60(2):212–25. https://doi.org/10.1016/j.compag.2007.08.003.

Sibley, Kevin J., Tessema Astatkie, Gordon Brewster, Paul C. Struik, John F. Adsett, and Kris Pruski. 2009. “Field-Scale Validation of an Automated Soil Nitrate Extraction and Measurement System.” Precision Agriculture 10(2):162–74. https://doi.org/10.1007/s11119-008-9081-1.

Singh, Mukul, Rajul S. Patkar, Madhuri Vinchurkar, and Maryam Shojaei Baghini. 2020. “Cost Effective Soil pH Sensor Using Carbon-Based Screen-Printed Electrodes.” IEEE Sensors Journal 20(1):47–54. https://doi.org/10.1109/JSEN.2019.2941695.

Sinha, S., R. Rathore, S. K. Sinha, R. Sharma, R. Mukhiya, and V. K. Khanna. 2014. “Modeling and Simulation of ISFET Microsensor For Different Sensing Films.” in ISSS International Conference on Smart Materials, Structures and Systems. Bangalore, India.

Smolka, M., D. Puchberger-Enengl, M. Bipoun, A. Klasa, M. Kiczkajlo, W. Śmiechowski, P. Sowiński, C. Krutzler, F. Keplinger, and M. J. Vellekoop. 2017. “A Mobile Lab-on-a-Chip Device for on-Site Soil Nutrient Analysis.” Precision Agriculture 1–17. https://doi.org/10.1007/s11119-016-9452-y.

Sohbati, Mohammadreza, and Christofer Toumazou. 2014. “A Temperature Insensitive Continuous Time ΔpH to Digital Converter.” Proceedings - IEEE International Symposium on Circuits and Systems 37–40. https://doi.org/10.1109/ISCAS.2014.6865059.

Sohbati, Mohammadreza, and Christofer Toumazou. 2015. “Dimension and Shape Effects on the ISFET Performance.” IEEE Sensors Journal 15(3):1670–79. https://doi.org/10.1109/JSEN.2014.2365291.

Tavares, Tiago Rodrigues, José Paulo Molin, Lidiane Cristina Nunes, Elton Eduardo Novais Alves, Fábio L. Melquiades, Hudson Wallace Pereira de Carvalho, and Abdul Mounem Mouazen. 2020. “Effect of X-Ray Tube Configuration on Measurement of Key Soil Fertility Attributes with XRF.” Remote Sensing 12(6). https://doi.org/10.3390/rs12060963.

Temple-Boyer, P., A. Benyahia, W. Sant, M. L. Pourciel-Gouzy, J. Launay, and A. Martinez. 2008. “Modelling of Urea-EnFETs for Haemodialysis Applications.” Sensors and Actuators, B: Chemical 131(2):525–32. https://doi.org/10.1016/j.snb.2007.12.037.

Templier, M., & Paré, G. (2015). A framework for guiding and evaluating literature reviews. Communications of the Association for Information Systems, 37. https://doi.org/10.17705/1CAIS.03706.

Tsukor, V., Hinck, S., Nietfeld, W., Lorenz, F., Najdenko, E., Möller, A., ... & Ruckelshausen, A. (2019). Automated mobile field laboratory for on-the-go soil-nutrient analysis with the ISFET multi-sensor module. In Proceedings 77th International Conference on Agricultural Engineering (AgEng 2019) (pp. 377-382).

Veris Technologies. 2018. "Veris On-the-Go Sensors." Retrieved November 20, 2018 (https://www.veristech.com/the-sensors).

Viscarra Rossel, R. A., and C. Walter. 2004. "Rapid, Quantitative and Spatial Field Measurements of Soil PH Using an Ion Sensitive Field Effect Transistor." Geoderma 119(1–2):9–20. https://doi.org/10.1016/S0016-7061(03)00219-2.

Viscarra Rossel, R. A., Adamchuk, V. I., Sudduth, K. A., McKenzie, N. J., & Lobsey, C. (2011). Proximal soil sensing: An effective approach for soil measurements in space and time. En Advances in Agronomy (Vol. 113, pp. 243-291). Elsevier. https://doi.org/10.1016/B978-0-12-386473-4.00005-1.

Welch, David, Sahil Shah, Sule Ozev, and Jennifer Blain Christen. 2013. "Experimental and Simulated Cycling of ISFET Electric Fields for Drift Reset." IEEE Electron Device Letters 34(3):456–58. https://doi.org/10.1109/LED.2013.2240648.

Wilson, Denise Michèle, Scan Hoyt, Jiri Janata, Karl Booksh, and Louis Obando. 2001. "Chemical Sensors for Portable, Handheld Field Instruments." IEEE Sensors Journal 1(4):256–74. https://doi.org/10.1109/7361.983465.

Wong, H. S., & White, M. H. (1988, December). A self-contained CMOS integrated pH sensor. In Technical Digest., International Electron Devices Meeting (pp. 658-661). IEEE. https://doi.org/10.1109/IEDM.1988.32899.

Xu, Zhen, Xinran Wang, Robert J. Weber, Ratnesh Kumar, and Liang Dong. 2017. "Nutrient Sensing Using Chip Scale Electrophoresis and In Situ Soil Solution Extraction." IEEE Sensors Journal 17(14):4330–39. https://doi.org/10.1109/JSEN.2017.2704918.

Yan, Liu, Pantelis Georgiou, Timothy G. Constandinou, David Garner, and Chris Toumazou. 2009. "An Auto-Offset-Removal Circuit for Chemical Sensing Based on the PG-ISFET." Proceedings - IEEE International Symposium on Circuits and Systems 1165–68. https://doi.org/10.1109/ISCAS.2009.5117968.

Yao, Ke, Yihua Zhu, Ping Wang, Xiaoling Yang, Pengzhi Cheng, and Hui Lu. 2007. "ENFET Glucose Biosensor Produced with Mesoporous Silica Microspheres." Materials Science and Engineering C 27(4):736–40. https://doi.org/10.1016/j.msec.2006.07.011.

Yin, H., Cao, Y., Marelli, B., Zeng, X., Mason, A. J., & Cao, C. (2021). Soil sensors and plant wearables for smart and precision agriculture. Advanced Materials, 33(20), 2007764. https://doi.org/10.1002/adma.202007764.

Zabrowski, Michat, Dariusz Szmiguel, and Piotr Grabiec. 2014. "BSC ISFET as Transcutaneous Blood Capnometry Sensor." HI Nation. Conf. of Nano a. Micromechanics. 801(11):142–46. https://doi.org/10.12915/pe.2014.11.39.